



Review

# Nitrate- and Nitrite-Sensing Histidine Kinases: Function, Structure, and Natural Diversity

Ivan Gushchin <sup>1,\*</sup>, Vladimir A. Alekseenko <sup>1</sup>, Philipp Orekhov <sup>1,2</sup>, Ivan M. Goncharov <sup>1</sup>, Vera V. Nazarenko <sup>1</sup>, Oleg Semenov <sup>1</sup>, Alina Remeeva <sup>1</sup> and Valentin Gordeliy <sup>1,3,4,5,\*</sup>

<sup>1</sup> Research Center for Molecular Mechanisms of Aging and Age-Related Diseases, Moscow Institute of Physics and Technology, 141700 Dolgoprudny, Russia; vladimir.alekseenko@phystech.edu (V.A.A.); orekhov@mail.bio.msu.ru (P.O.); ivan.goncharov@phystech.edu (I.M.G.); nazarenko@phystech.edu (V.V.N.); semenov.oyu@phystech.edu (O.S.); alina.remeeva@phystech.edu (A.R.)

<sup>2</sup> Faculty of Biology, M.V. Lomonosov Moscow State University, 119991 Moscow, Russia

<sup>3</sup> Institut de Biologie Structurale J.-P. Ebel, Université Grenoble Alpes-CEA-CNRS, 38000 Grenoble, France

<sup>4</sup> Institute of Biological Information Processing (IBI-7: Structural Biochemistry), Forschungszentrum Jülich, 52428 Jülich, Germany

<sup>5</sup> JuStruct: Jülich Center for Structural Biology, Forschungszentrum Jülich, 52428 Jülich, Germany

\* Correspondence: ivan.gushchin@phystech.edu (I.G.); g.valentin@fz-juelich.de (V.G.)



**Citation:** Gushchin, I.; Alekseenko, V.A.; Orekhov, P.; Goncharov, I.M.; Nazarenko, V.V.; Semenov, O.; Remeeva, A.; Gordeliy, V. Nitrate- and Nitrite-Sensing Histidine Kinases: Function, Structure, and Natural Diversity. *Int. J. Mol. Sci.* **2021**, *22*, 5933. <https://doi.org/10.3390/ijms22115933>

Academic Editors: Xavier Latour and Corinne Barbey

Received: 12 April 2021

Accepted: 28 May 2021

Published: 31 May 2021

## 1. Introduction

Microorganisms live in variable environments that require rapid reaction to changing conditions. Consequently, they developed a number of signaling systems that are classified according to the number of distinct molecular entities involved in signal transduction: one-component systems (OCS), two-component systems (TCS), and so on. While OCS usually respond to intracellular stimuli, TCS are able to detect extracytoplasmic molecules by means of a membrane-spanning receptor that transmits the signal inside the cell and controls the activity of its respective soluble response regulator (RR).

Due to their versatility and variety of the recognized signals, TCS are widespread among microorganisms: bacterial genomes often encode tens and sometimes more than a hundred receptor and RR genes [1–5]. Usually, there are slightly more RR genes than receptor genes, and sometimes, a single receptor may regulate the activity of different RR proteins [3,6,7]. TCS may respond to ions, gases, small molecules, peptides, and other chemicals as well as to factors such as temperature, osmolarity, membrane fluidity, or illumination [8–11]. Since many of them are important for bacterial survival and pathogenicity,



**Copyright:** © 2021 by the authors. Licensee MDPI, Basel, Switzerland. This article is an open access article distributed under the terms and conditions of the Creative Commons Attribution (CC BY) license (<https://creativecommons.org/licenses/by/4.0/>).

TCS constitute promising targets for antimicrobial treatments [12–14]. TCS receptors are also often used in synthetic biology, in engineered proteins and cellular networks [15–19], as well as whole cell biosensors [20–22].

Regulation of RR activity is usually achieved via its phosphorylation or dephosphorylation by a cognate histidine kinase (HK) [23,24]. Depending on the signal, HK interconverts between the kinase and phosphatase states. In the kinase state, HK transfers the phosphate from ATP to its own histidine amino acid and then to the RR's aspartate. Hybrid HKs may also contain additional receiver and histidine phosphotransfer domains, which eventually pass the phosphate to the RR. In the phosphatase state, HK dephosphorylates the RR. Usually, HK dynamically interconverts between the two states, and the presence of the ligand biases the equilibrium toward the kinase state [25].

There are three major types of TCS, which are based on sensory HKs, chemoreceptors, and sensory rhodopsins. HKs are usually dimeric proteins that perceive the signal and act on RR directly; RRs often regulate transcription and intracellular processes [23,24,26]. Chemoreceptors and sensory rhodopsin-based photoreceptors are involved in chemo- and phototaxis, but they can also perform other functions [10,11,27,28]. They form higher-order assemblies composed of trimers-of-dimers of the receptor proteins in complex with the histidine kinase CheA and accessory proteins [27,29]; the activity of CheA is regulated by the receptors [30]. Whereas HKs generally control cellular physiology, chemoreceptors and photoreceptors are mostly responsible for taxis. Sensory proteins usually either span the cell membrane or are anchored to it. However, numerous examples of the cytoplasmic receptors also exist [2,31–33], which sense intracellular signals or ligands capable of passive diffusion across the plasma membrane.

HKs have highly variable modular architectures that, in the minimal form, include the sensor domain, dimerization and histidine phosphotransferase (DHp) domain, and catalytic (CA) domain. They can also contain a transmembrane (TM) domain and additional signal transduction domains [34] such as HAMP (domain found in histidine kinases, adenylyl cyclases, methyl-accepting proteins, and phosphatases [35–37]), PAS (Per-ARNT-Sim [38,39]), and GAF (found in cGMP-specific and stimulated phosphodiesterases, adenylate cyclases, and FhlA [40]), which may or may not be sensors themselves. Exemplary architectures of sensory HKs may be found in thematic reviews [8,9,32,37,41]. Sensory domains are predominantly either fully  $\alpha$ -helical (such as 4-helical bundle, 4HB fold) or mixed  $\alpha/\beta$  (such as single and double Cache) [42,43]. Conformational changes in different sensory domains are likely to be similar, because they are often interchangeable, and functional chimeric sensor proteins are often easily constructed [44–52]. Sometimes, more than one signal may be recognized, either by the same sensory domain [53,54] or by the canonical sensory domain and additional cytoplasmic modules [55,56]. Finally, atypical signaling modes are also observed for some HKs [57]. In general, signal transduction is achieved via conformational coupling of the domains to each other [23,25,37,41,58,59].

In this review, we focus on bacterial nitrate- and nitrite-sensing HKs (NSHKs), which are among the best studied TCS. In particular, we review the function of NSHKs, analyze their natural diversity, and describe the available structural information.

## 2. Microbial Nitrate and Nitrite Respiration and Respective Sensor Proteins

Many bacteria can use nitrate or nitrite as an electron acceptor for respiration [60–64]. Overall, microbial nitrogen cycling is an important topic. Marine and terrestrial bacteria carry out nitrogen fixation, nitrification, and denitrification and thus strongly affect the distribution of environmental nitrogen compounds: nitrate, nitrite, nitric oxide, nitrous oxide, dinitrogen gas, hydroxylamine, hydrazine, and ammonia [62,63]. In particular, they affect the emission of nitrous oxide ( $N_2O$ ), an ozone-depleting greenhouse gas [65]. Microbial populations in the mammalian gut and mouth utilize nitrous compounds for colonization [66,67] and survival during inflammation [68], and they can affect the host's nitrate metabolism as well [69]. An anaerobic endosymbiont that generates energy for a ciliate host by denitrification was discovered recently [70].

Consequently, the bacteria need the means to sense nitrates and nitrites and respond to them. Currently, several different microbial nitrate sensors have been identified and characterized. NarQ and NarX from *Escherichia coli* are prototypical nitrate-responsive HKs, transmembrane proteins that are members of NarQP and NarXL TCSs, respectively [71]. NarS is a histidine kinase with the cognate response regulator NarL, which is related to that of the NarXL system; NarS is predicted to have six TM segments and was found to be necessary for nitrate regulation in *Mycobacterium tuberculosis* [72]. NreA from *Staphylococcus carnosus* is a soluble protein with a GAF domain fold that regulates the activity of oxygen-sensing NreBC TCS [73]. McpN is a recently identified chemoreceptor that is responsible for nitrate chemotaxis in *Pseudomonas aeruginosa* PAO1 [74]. Finally, NasR is a nitrate-responsive transcription antiterminator from *Klebsiella oxytoca* (belongs to *Gammaproteobacteria*) [75], which contains NIT (nitrate- and nitrite-responsive domain [76]) and ANTAR (RNA-binding domain from AmiR and NasR transcription antitermination regulators [77]). Interestingly, McpN, NarQ, NarX, and NasR bind nitrate in a similar way [78], despite little to no similarity between residues that do not participate directly in ligand binding.

### 3. NarQ/NarX-Like Nitrate- and Nitrite-Sensing TCSs

The genes responsible for nitrate regulation were identified early on by screening for regulation-compromised mutants of *Escherichia coli* [79]. First, the NarL-mutant was shown to lack a nitrate-specific positive regulation [80] and the respective gene product to activate the nitrate reductase operon and repress the fumarate reductase and trimethylamine N-oxide reductase operons [81]. Later, the first histidine kinase gene, NarX, responsible for nitrate regulation in *E. coli* was discovered, and NarX and NarL were shown to form an HK-RR pair [82–84]. Soon thereafter, it was revealed that the *E. coli* genome harbors a second HK involved in nitrate regulation, named NarQ [85,86], and its cognate RR, NarP [87]. In the *E. coli* genome, *narX* is adjacent to *narL*, but *narQ* and *narP* are separate from each other and from *narXL*. However, cross talk between the two systems is also observed (Figure 1 [88]). Given that NarX responds only to nitrate ( $\text{NO}_3^-$ ), and NarQ responds both to nitrate and nitrite ( $\text{NO}_2^-$ ), cross talk allows for differential regulation of the output depending on the concentration of the two ions [88]. Thus, both nitrate-responsive TCSs are required for efficient nitrate regulation in *E. coli*. In addition to the *nar* (nitrate reductase) operon, NarQ and NarX also regulate several other metabolism-related operons such as *nir* (nitrite reductase), *nap* (periplasmic nitrate reductase), *frd* (fumarate reductase), *dcu* (dicarboxylate uptake), or *dms* (dimethylsulphoxide reductase) (Figure 1 [88,89]).

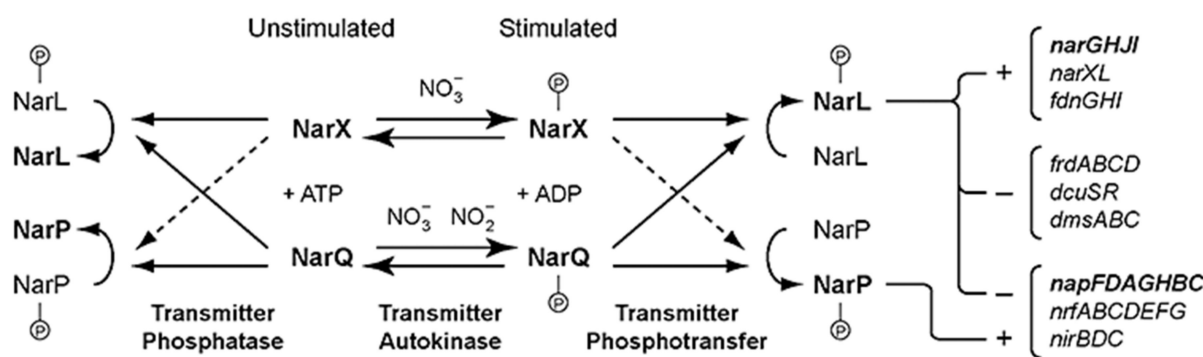


**Figure 1.** Model for the NarX–NarL and NarQ–NarP cross-regulation network. Dashed arrows represent relatively slow reactions. The NarX and NarQ sensor populations are hypothesized to be in a two-state equilibrium determined by stimulus (ligand binding). Phospho-sensors catalyze response regulator phosphorylation, whereas dephospho-sensors catalyze regulator dephosphorylation. Phospho-regulators activate (+) or repress (−) transcription; representative target operons are shown. Reproduced with permission from the reference [88].

In addition to NarXL and NarQP from *E. coli*, similarly functioning systems from *Haemophilus influenzae* [71,90] *Pseudomonas stutzeri* [91], *Pseudomonas aeruginosa* [92,93], *Neisseria gonorrhoeae* [94,95], *Shewanella oneidensis* [96], *Burkholderia thailandensis* [97], and *Burkholderia pseudomallei* [98] were probed experimentally. With the advances in sequencing, several more HKs were identified in Beta- and Gammaproteobacteria [71]. However, since the time of the latter analysis, tens of thousands of new bacterial genomes [99] and metagenomes [100] have been sequenced, resulting in the explosive growth of respective databases [101,102]. Below, we analyze the currently available genomic information.

#### 4. Natural Diversity of Nitrate- and Nitrite-Sensing Histidine Kinases

*E. coli* NarQ and NarX have an amino acid identity of ≈29.4%, whereas NarP and NarL are ≈44.4% identical. Both *E. coli* NarQ and NarX consist of seven clearly defined structural elements: sensor domain, transmembrane region, HAMP domain, signaling helix, GAF-like, DHp, and CA ([37], detailed descriptions of the domains are presented in the following sections). Of these seven elements, six are not specific to nitrate receptors, and only the sensor domain is the defining feature of microbial nitrate and nitrite sensor histidine kinases. Consequently, we used InterPro [103] to retrieve histidine kinase genes with the characteristic NarQ/NarX-like sensor domain that presumably encodes functional NSHKs. This sensor domain is labeled “NarX-like, N-terminal” in the database, and it has an identifier IPR029095. On 14 January 2021, InterPro v. 83.0 contained information about ≈12,000 proteins with this domain. Some of these proteins were clearly chemoreceptors, since they also comprised the MCP domain (“Methyl-accepting chemotaxis protein (MCP) signaling domain”, identifier IPR004089). Others are clearly histidine kinases, having the DHp (“Signal transduction histidine kinase, subgroup 3, dimerization, and phosphoacceptor domain”, identifier IPR011712) and CA (“Histidine kinase/HSP90-like ATPase”, IPR003594) domains.

We note that some of the signal transduction domains are very variable and are not always easy to recognize in the sequence. For both *E. coli* NarQ and NarX (UniProt accession codes P27896 and P0AFA2), InterPro contains the information only about the sensor, TM, HAMP, DHp, and CA domains, while the S-helix and GAF-like domains are not recognized (not annotated). Consequently, while searching for NSHKs in InterPro, we obtained the sequences with several architectures with the assumption that some of the other domains may be not recognized as well. We found 4952 sequences with the architecture “sensor, HAMP, DHp, and CA”, 582 sequences with the architecture “sensor, HAMP, GAF, DHp, and CA”, 303 sequences with the architecture “sensor, DHp, and CA”, and 284 with the architecture “sensor, HAMP, and DHp”. These sequences were pooled together into a single set containing 6121 different records, which was used for the downstream analyses.

Phylogenetic analysis reveals that the obtained sequences form several large and several smaller clusters as well as some isolated sequences. NarQ and NarX are grouped with the genes from Beta- and Gammaproteobacteria, including a subgroup of various sulfur-reducing bacteria (Figure 2). Two other large clusters are also prominent: one contains mostly Betaproteobacteria (*Burkholderiales* and *Neisseriales*), and another contains *Bacteroidetes* (Figure 2). Finally, a distinct set of *Chloroflexi* sequences is also observed, including the genes from *Litorilinea aerophila* (GenBank ID OUC06986.1, unpublished), *Caldilinea aerophila* [104], and *Aggregatilinea lenta* [105], as well as numerous genes belonging to anaerobic ammonium oxidation (anammox) bacterial community members [106–115] such as *Candidatus Denitrolinea symbiosum* [116].

Since the sequences of the genes from the latter clusters have diverged from the known nitrate sensors, we analyzed the genetic neighborhoods of several representative NSHKs from the following species: *Escherichia coli*, *Pseudomonas aeruginosa*, endosymbiont of *Riftia pachyptila*, *Thiobacillus denitrificans*, *Neisseria meningitidis*, *Paraburkholderia graminis*, *Burkholderia pseudomallei*, *Aggregatilinea lenta*, *Haemophilus influenzae*, *Vibrio cholerae*, *Joostella marina*, *Indibacter alkaliphilus*, and *Thermoflexibacter ruber*. We observe that almost all of these

genes contain other nitrate/nitrite-related genes in the vicinity (*narK*, *narGHJI*, *nap*, *nir*, *nos* or *nrt* [117]), supporting the assignment to nitrate/nitrite-sensing histidine kinase family (Figure 3).

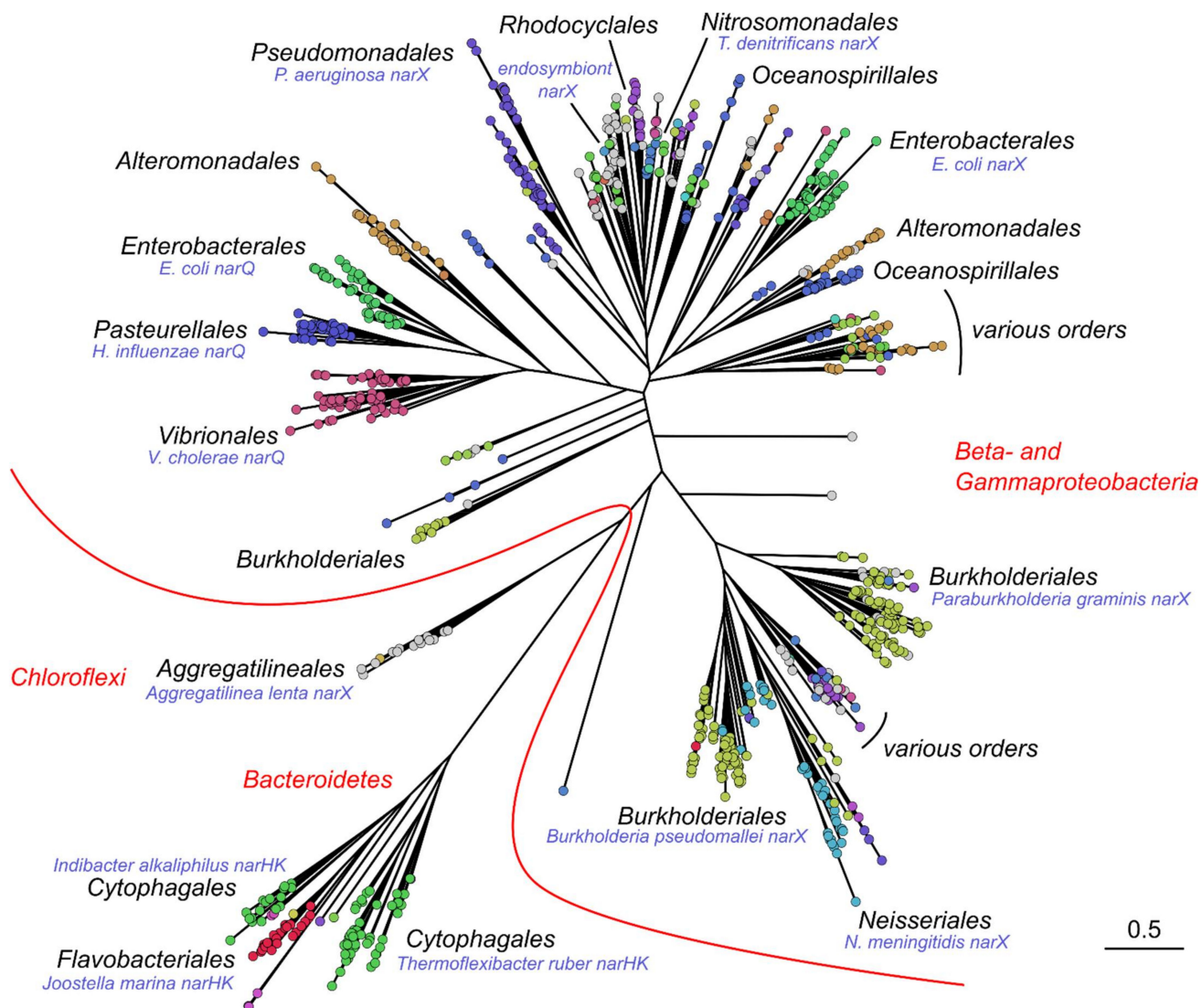


**Figure 2.** Phylogenetic tree of nitrate- and nitrite-sensing histidine kinases. Genes belonging to different bacterial orders are shown in different colors; genes with missing order information are shown in gray. Genomic neighborhoods of representative genes (labeled in blue) are shown in Figure 3. The tree was calculated for a set of 920 representative genes (centroids from clustering at the 80% sequence identity level using UCLUST [118]) using FastTree 2 [119] and drawn using FigTree [120]. Multiple sequence alignment, taxonomic annotation and phylogenetic tree for the analyzed NSHK sequences are available as Supplementary Datasets 1, 2 and 3.

As described above, the *E. coli* genome contains two NSHK genes, *narQ* and *narX*, with amino acid identity of  $\approx 29.4\%$ . We used CD-HIT [121] to cluster the genes ascribed to each bacterial species separately, and we found  $\approx 800$  strains and species having two NSHK genes with less than 75% sequence identity and  $\approx 2100$  strains and species with a single NSHK gene (Figure 4). Two NSHK genes per genome are mostly observed in *Enterobacterales*, although examples from other bacterial orders are also observed (Figure 4). Whereas in most of the organisms with a single NSHK gene, the gene is more similar to *narX*, *narQ*-like-only organisms are also observed. We note that the obtained numbers are approximate, since the available genomic data do not have uniform quality. The proportion between the two types of organisms is also approximate, because bacterial species are

sequenced nonuniformly. For example, hundreds of *Escherichia coli* and *Salmonella enterica* genomes are available, but for some other genera, the data is scarce. At the same time, we did not find any reliable examples of organisms having more than two NSHK genes with pairwise sequence identity of less than 75%.

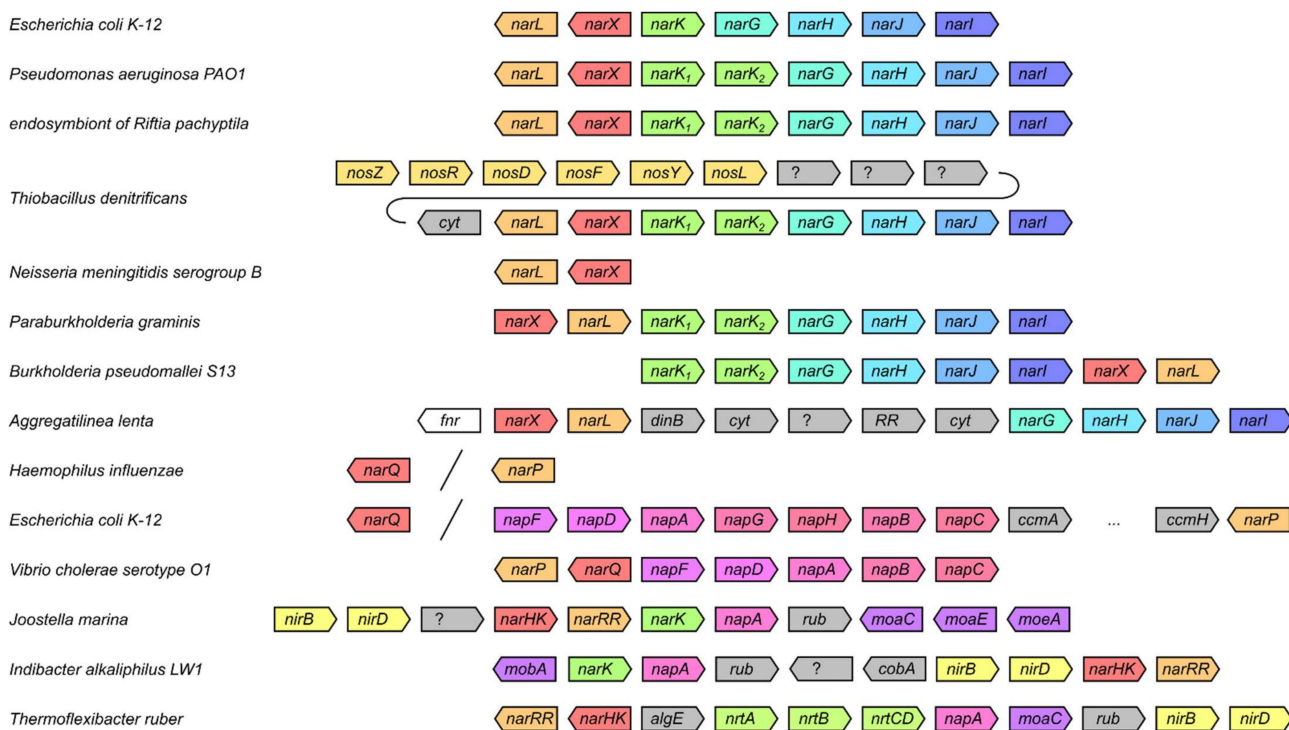


**Figure 3.** Order of putative nitrate metabolism genes in representative genomes (GenBank IDs U00096.3, AE004091.2, AFOC01000011.1, CP000116.1, CP001561.1, CADIKA01000002.1, CH899769.1, NZ\_BFCB01000003.1, L42023.1, CP000626.1, JH651379.1, ALWO02000023.1, FONY01000003.1). *Bacteroidetes* genes are labeled *narHK* and *narRR*, since they are notably different from *narQ/narP* and *narX/narL*, and the architectures of the sensor proteins are different (GAF-like domains are absent). No genes possibly involved in nitrate metabolism are observed in the vicinity of *Escherichia coli* *narQ*, *Haemophilus influenzae* *narQ*, and *narP* and *Neisseria meningitidis* *narX* and *narL*. *narK<sub>1</sub>* and *narK<sub>2</sub>* are sometimes annotated in the literature as *narK* and *narT*, respectively. *nrtB/C* are sometimes referenced to as *ntrB/C*; here, these genes are representatives of the ATP-Binding Cassette (ABC) transporters family that are involved in nitrate transport and are not the members of the *ntrBC* TCS, which controls expression of the nitrogen-regulated (*ntr*) genes in response to nitrogen limitation [122,123]. *mobA* encodes molybdopterin-guanine dinucleotide biosynthesis protein [124–126]; *moaC* encodes cyclic pyranopterin monophosphate synthase [127], which is a nitrate reductase and molybdopterin biosynthesis-associated protein; molybdopterin guanine dinucleotide is a cofactor for nitrate reductases [124,128,129]. The genes whose possible involvement into nitrate metabolism is not clear are colored gray; *rub*, rubredoxin; *cyt*, c-type cytochrome.

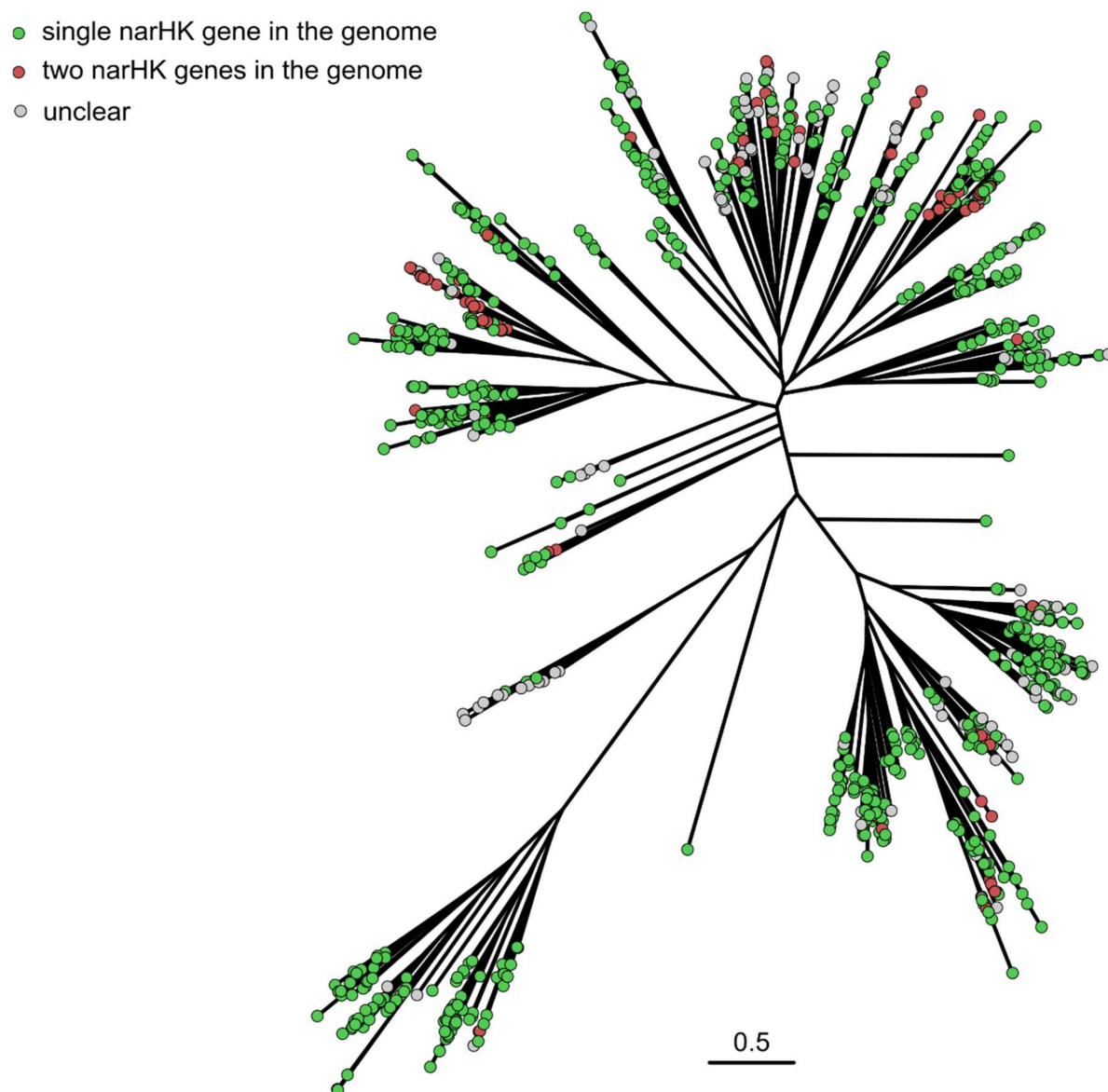


**Figure 4.** Singlet and doublet NSHK genes in the assembled dataset. The phylogenetic tree is the same as in Figure 2. Sequences belonging to genomes with a single NSHK are shown in green and those belonging to genomes with two NSHKs are shown in red. Metagenomic sequences and sequences without assigned strain are shown in gray.

##### 5. Architecture of Nitrate- and Nitrite-Sensing Histidine Kinases

NarQ and NarX from *Escherichia coli* are 566 and 598 amino acid long and have molecular weights of 63.7 kDa and 67.1 kDa, respectively. Both have identical architecture, form dimers under physiological conditions, and consist of seven domains: the periplasmic sensor domain, the TM domain, and five cytoplasmic domains—HAMP, signaling helix (S-helix), GAF-like, DHp, and CA (Figure 5).

Multiple sequence alignment reveals remarkable conservation of the overall features of IPR029095-containing proteins. Most sequences are encoding full-length proteins with all of the seven domains intact. Yet, in some of the proteins, the region between the TM helices and the DHp domain is shortened. For example, in *E. coli* NarQ, it is  $\approx$ 30 amino acids shorter than in NarX. A similar decrease in the length of this region is also observed for genes from *Enterobacteriales*, *Pasteurellales*, *Vibrionales*, and *Alteromonadales* that are clustering close to *E. coli* narQ (Figure 2) but not for other proteobacterial genes. The proteins from the separate *Burkholderiales* and *Neisseriales* cluster are 15–20 amino acids shorter compared to

*E. coli* NarX. Yet the most surprising observation is that the TM-DHp region is even shorter in the proteins from the *Bacteroidetes* cluster (Figure 2). Careful examination (secondary structure analysis and homology modeling performed using RaptorX [130] and SWISS-MODEL [131]) reveals that the *Bacteroidetes* NSHKs lack the HAMP and GAF-like domains. *Flavobacteriales* and *Cytophagales* proteins clustering with the *Indibacter alkaliphilus* HK have a PAS domain, whereas in the *Cytophagales* proteins clustering with the *Thermoflexibacter ruber* HK, the TM domain is directly connected to the DHp domain by a continuous  $\alpha$ -helix (Figure 5). Based on the gene ordering (Figure 3) and architecture of the nitrate sensors (Figure 5), we suggest that NSHKs may be grouped into three classes: (i) shorter diverging *Bacteroidetes* sensors; (ii) NarQ-like proteins from *Enterobacterales*, *Pasteurellales*, *Vibrionales*, and *Alteromonadales*, clustering close to *E. coli narQ*; and (iii) NarX-like proteins: all other NSHKs.

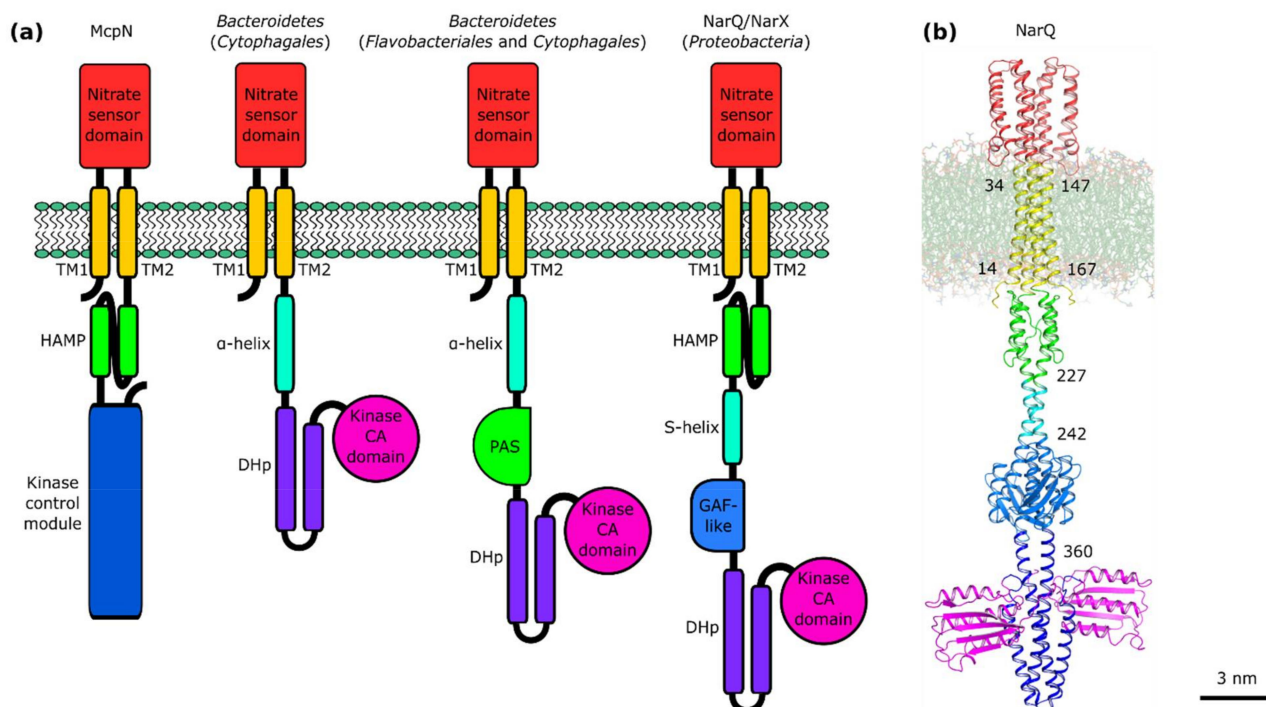


**Figure 5.** Architecture of transmembrane nitrate sensors. (a) Architecture of nitrate-responsive TCS receptors: chemoreceptor McpN and different nitrate/nitrite sensor HKs: GAF-less proteins from *Bacteroidetes* and NarQ and NarX from *Proteobacteria*. Panel adapted from [37]. (b) Atomic model of NarQ in a realistic membrane. The protein is a homodimer. The numbers indicate the respective amino acid numbers at the domain junctions.

Given the high level of the overall amino acid sequence conservation, including the nitrate-binding motif and the residues important for phosphorylation, we presume that all these sequences encode mostly functional NSHKs. We analyzed how well the individual domains are conserved and found notable variation. Sensor and HAMP domains generally vary to the same degree as the whole protein; TM  $\alpha$ -helices and the region corresponding to the GAF-like domain are less conserved, whereas the catalytic domain and especially S-helix and DHp are conserved better than the protein overall (Figure 6).

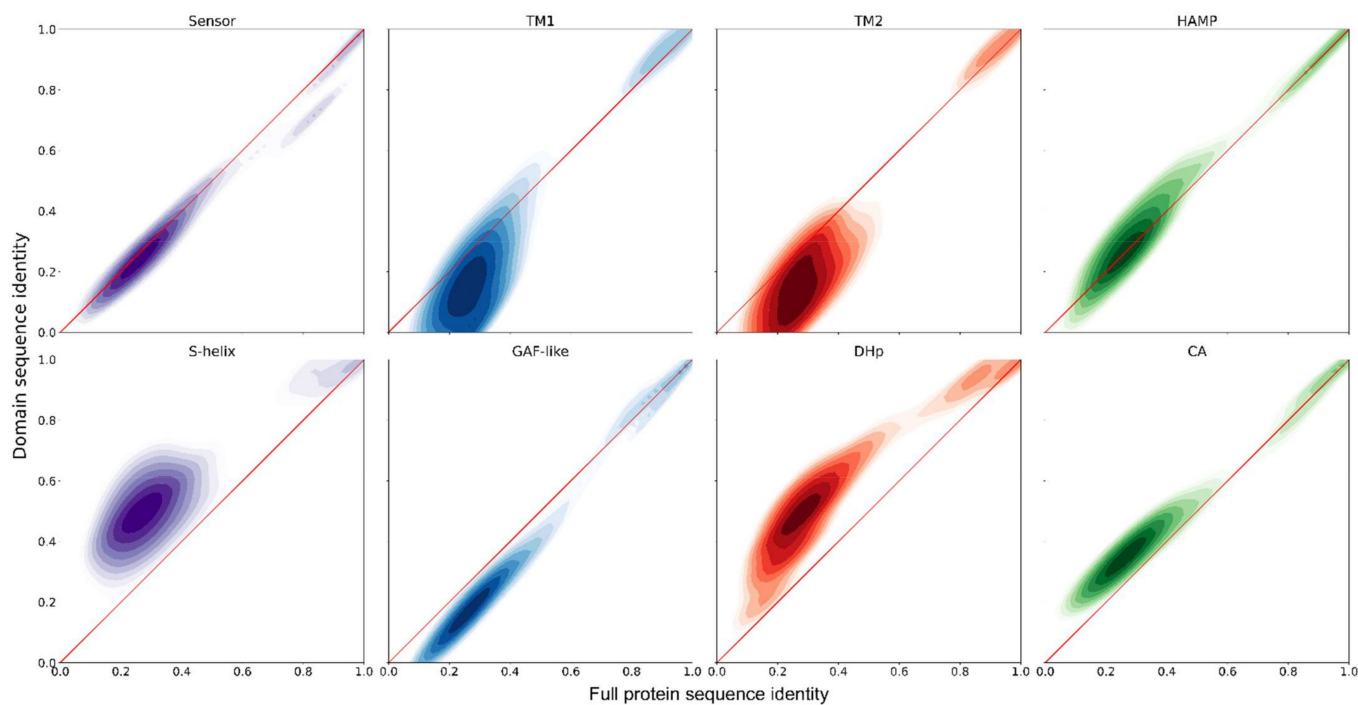


**Figure 6.** Conservation of NSHK domains relative to conservation of the whole protein. Shown are pairwise sequence identity values for all NSHKs in the dataset smoothed with Gaussian kernel density estimation and transformed to logarithmic scale. Red diagonals are used as guides: the values above the diagonals correspond to better domain conservation compared to the whole protein, whereas the values below the diagonals correspond to lower relative domain conservation.

## 6. Structure of Nitrate- and Nitrite-Sensing Histidine Kinases

Most sensor HKs are complex dynamic multi-domain proteins. While full-length structures of several soluble sensor HKs have been determined previously [132,133], no experimental structure of a full-length TM HK is available at the moment. This presumably is the consequence of the proteins being membrane-associated as well as very flexible and dynamic. Similarly, no high-resolution structures are available for chemoreceptors or sensory rhodopsin-transducer complexes, although low-resolution electron microscopy models have been obtained [27,29,134–137].

In the absence of full-length structures of TCS, a divide-and-conquer approach has been very fruitful: structures of different domains are determined individually, and then, the model of the whole protein is assembled from parts. In particular, a plethora of sensor domain structures are known at the moment that highlight many different modes of ligand binding: symmetric, asymmetric, at the dimerization interface, and reveal signaling-associated conformational changes [10,25,37,42,138]. The other domains have also been well characterized, possibly with the exception of the TM module [23,25,37,41,58].

Below, we review what is known about each NSHK domain. NSHKs, having seven domains, are more complex compared to many other HKs. Experimentally determined structures are currently available for the sensor, TM, and HAMP domains [78,139–141]. We used homology modeling to prepare atomic models of other domains and built a computational model of full-length NarQ (Figure 5b). The size of the full-length NarQ dimer is roughly  $24 \times 9$  nm; it is quite remarkable that the signal (binding of the ligand to the sensor domain) can be reliably transmitted to the DHp and CA domains 200 Å away on the other side of the membrane. Structural details and specifics of signal transduction by each of the domains will be presented below in the context of natural diversity of the proteins.

## 7. Sensor Domain of Nitrate- and Nitrite-Sensing Histidine Kinases

The sensor domain of NSHKs is responsible for binding the ligand (nitrate or nitrite) and transmitting the signal downstream. It is located in the extracytoplasmic space, preceded and followed by TM  $\alpha$ -helices (Figure 5). Earlier studies highlighted the similarity between the TM1-proximal regions of the NarQ and NarX periplasmic sensor domains [85,86]. The conserved sequence was called the “P-box” and shown to be important for nitrate sensing and nitrate–nitrite discrimination by NarQ and NarX [142–144].

Crystallographic structures of the nitrate sensor domain in the ligand-free and nitrate-bound forms have been determined both for *E. coli* NarQ and NarX (Figure 7, [139,140]). The sensor domain is mostly symmetric in both states and, as in many other TCS receptors, it is formed by four  $\alpha$ -helices H1–H4, with the ligand binding site at the dimerization interface between the helices H1 of the two protomers. The nitrate ion is coordinated by arginine side chains and stacked between glycine backbone atoms (Figure 8). The mutation of arginine to other amino acids, including lysine, resulted in a ligand-insensitive phenotypes [142–144]. The binding of nitrate causes rotation of the helices H1 and rearrangement of the TM domain-facing termini [139–141]. A similar nitrate binding mode is also observed in the nitrate chemoreceptor McpN [74] (architecture shown in Figure 5).

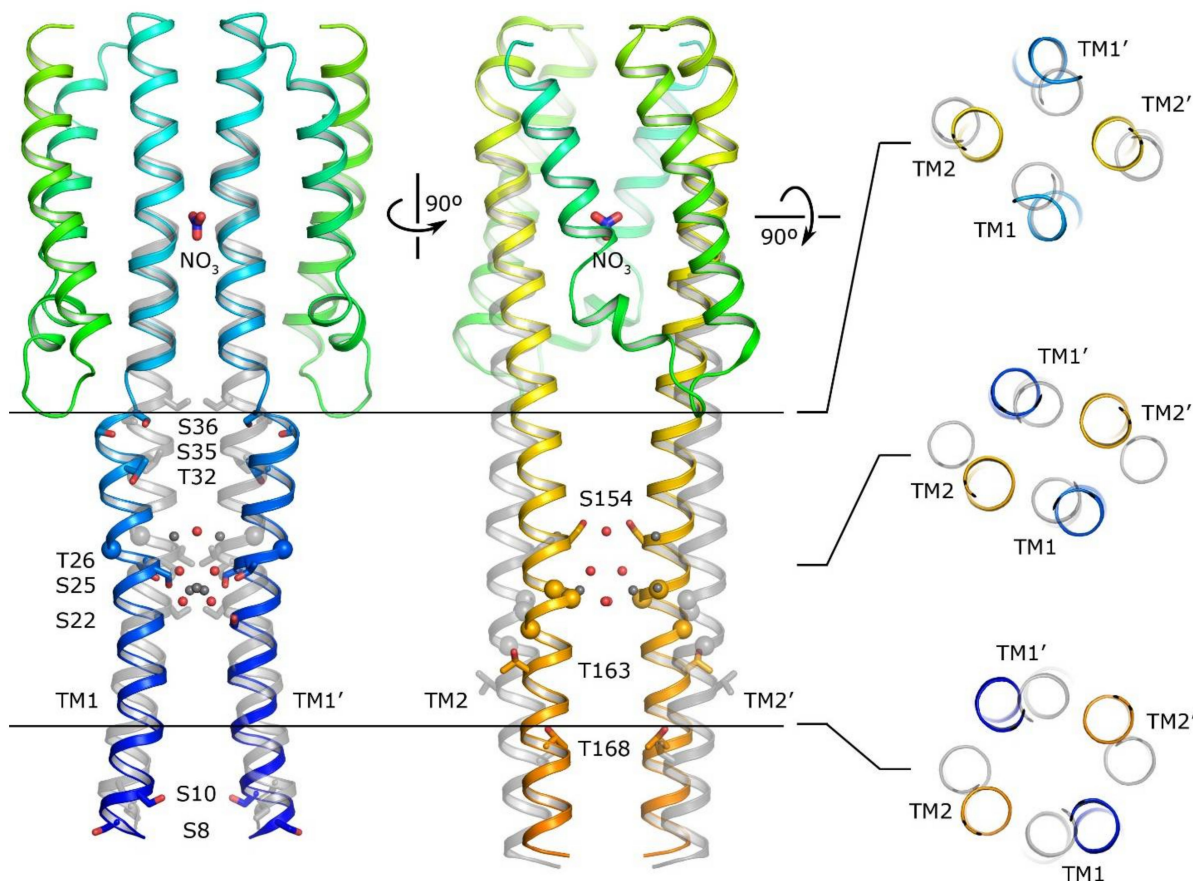


**Figure 7.** Signaling-associated conformational changes in the NarQ sensor and TM domains. Superposition of the symmetric ligand-free structure (gray) and symmetric ligand-bound structure (colored) is shown. The binding of nitrate causes downward displacement of TM1 and upward displacement of TM2, alongside with rearrangements in the membrane plane. **Left:** Changes in the conformation of helix TM1. **Center:** Changes in the conformation of helix TM2. **Right:** Changes in the arrangement of the TM helices. Serine and threonine side chains are shown explicitly, glycine C $\alpha$  atom positions are marked with spheres. Positions of water molecules in the TM region are shown with gray (apo) or red (holo) spheres. The structures are aligned by the sensor domains. Adapted from [140].

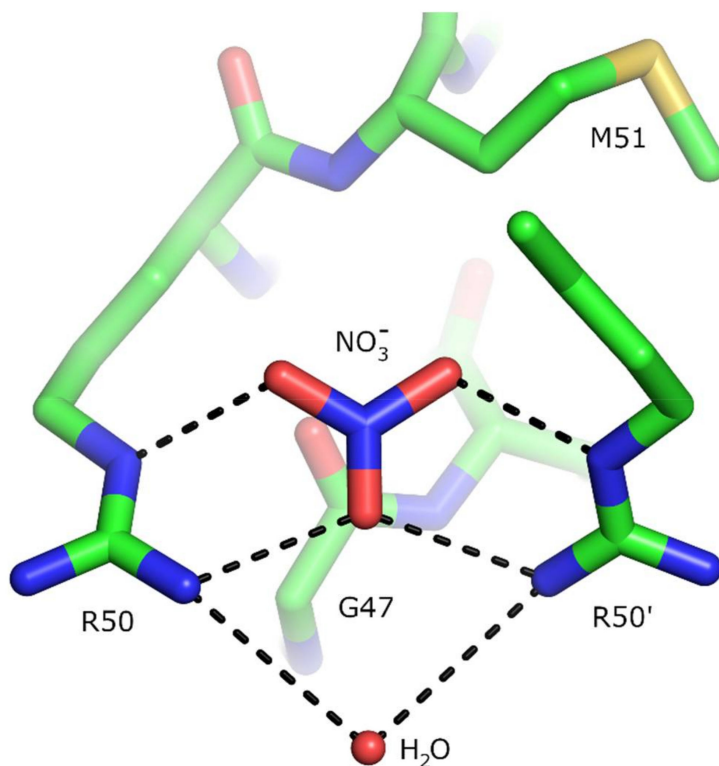


**Figure 8.** Structure of the nitrate-binding pocket in NarQ [140]. The nitrate is coordinated by Arg50 side chains of the two protomers and stacks with Gly47. The interaction may also be stabilized by interaction between the partially negatively charged carbonyl oxygen atoms of Gly47 and the partially positively charged nitrogen atom of the nitrate ion. G47 and R50 form the G-x-x-R motif conserved among many nitrate-responsive sensor proteins.

The characteristic motif for the nitrate-binding region of NSHKs, determined from the set of sequences that we obtained, is A<sub>77</sub>-I<sub>71</sub>-N<sub>99</sub>-x-A<sub>77</sub>-G<sub>100</sub>-S<sub>66</sub>-L<sub>77</sub>-R<sub>100</sub>-M<sub>91</sub>-Q<sub>54</sub>-S<sub>57</sub>-Y<sub>66</sub>-R<sub>72</sub>-L<sub>54</sub>, where the subscripts indicate the probability of observing the respective amino acid at this position (in percent). Evidently, the P-box is extremely well conserved among NSHKs. The nitrate-binding amino acids, forming the motif G-x-x-R (Figure 8), are also conserved among the nitrate-responsive chemoreceptors [74] and are partially conserved in the transcription antiterminator NasR, where both of the arginines are present, but one of the glycines is replaced with a glutamine in the asymmetric nitrate binding site [75].

#### 8. Transmembrane Domain of Nitrate- and Nitrite-Sensing Histidine Kinases

In the TCS receptors with an extracytoplasmic sensor domain, the TM domain serves as the link and the signal transducer between the sensor and the cytoplasmic domains. Usually, the TM domain consists of two TM  $\alpha$ -helices, TM1, which is N-terminal relative to the sensor domain, and TM2, which is C-terminal relative to the sensor domain [37], and NSHKs are not an exception to this rule (Figure 5).

Transmembrane proteins make a difficult target for experimental structural biology methods, because they need to be solubilized during purification and handled with special precautions thereafter [145–148]. Consequently, the amount of direct structural data on TM domains for any TCS receptor is currently limited compared to the data on other domains [37].

At the moment, only the structure of the NarQ, and not NarX, TM domain is available [78,140,141]. The only other known X-ray structure of the TM domain of a TCS receptor is that of sensory rhodopsin transducer [149–151]. Additionally, NMR models of TM domains of sensor HKs ArcB, QseC, and KdpD in monomeric forms are available [152]. Complementary methods such as mutagenesis, electron microscopy, modeling, and cysteine scan-

ning may provide valuable information on the TM domains [29,37,136,137,141,153–156], but they can also miss some intricate details of signaling-associated conformational changes.

The NarQ TM domain is arranged as a four-helical antiparallel coiled coil (Figure 5). While the TM bundle is usually symmetric (Figure 7), an asymmetric nitrate-bound form has also been observed [140]. The binding of nitrate causes rotation of the sensor domain  $\alpha$ -helix H1, which in turn leads to disruption of the  $\alpha$ -helical structure in the H1-TM1 junction and rearrangement of the sensor-proximal parts of TM helices (Figure 7, [140,141]). This is followed by overall twisting of the TM bundle and displacement of the TM helices in opposite directions (TM1 toward the cytoplasm and TM2 away from it). The latter conformational changes lead to restructuring of the HAMP domain and transduction of the signal downstream.

Interestingly, while TM  $\alpha$ -helices are often expected to be rigid and hydrophobic, this is not exactly the case for nitrate sensors. Indeed, the TM domain of NarQ contains several serines and threonines. Most of them are oriented toward the interior of the helical bundle and coordinate water molecules trapped in the resulting polar cavities (Figure 7 [140]). There is also one glycine amino acid in TM1 and three in TM2 (Figure 7); the helices bend around the glycines during the signal transduction [37]. Having obtained a set of nitrate-sensing histidine kinase sequences, we were interested to analyze whether these amino acids are conserved in this protein family.

Multiple sequence alignment shows no gaps between TM1 helices and the ligand-binding residues of the sensor domain's helix H1, as well as no gaps between the TM2 helices and the beginning of the cytoplasmic region (HAMP domain's helix AS1 in most of the genes). This fact underlies the importance of the respective junctions for signal transduction and allows us to analyze the amino acid frequencies in the TM region (Figures 9 and 10). Overall, amino acids in the NSHK TM domain are less well conserved (Figure 6). It seems that the sequences are not restrained by any particular interactions and are thus free to evolve as long as they remain mostly hydrophobic. Yet, surprisingly, we find that each TM helix contains on average one to two glycines and three to four serines or threonines (Figures 9 and 10). Analysis of amino acid frequencies at each TM helix position in the multiple sequence alignment reveals striking patterns of hydrophobic and hydrophilic side chains (Figure 9). Glycines, especially abundant in TM1, are separated by one, two, or four other amino acids and seemingly never form the G-x-x-x-G motif often observed in interacting TM helices [157,158]. Serines and threonines are even more plentiful and likely facilitate the assembly of the TM bundle [159,160]. Thus, we conclude that the presence of polar residues and water-filled cavities in the TM region of NarQ is not an artefact of this particular protein but rather a general feature of NSHKs, which is required for efficient folding and signal transduction. Glycines in TM helices were also found to be important for *E. coli* DcuS signaling [161], and similar conclusions have been reached for another *E. coli* histidine kinase, PhoQ [162,163].

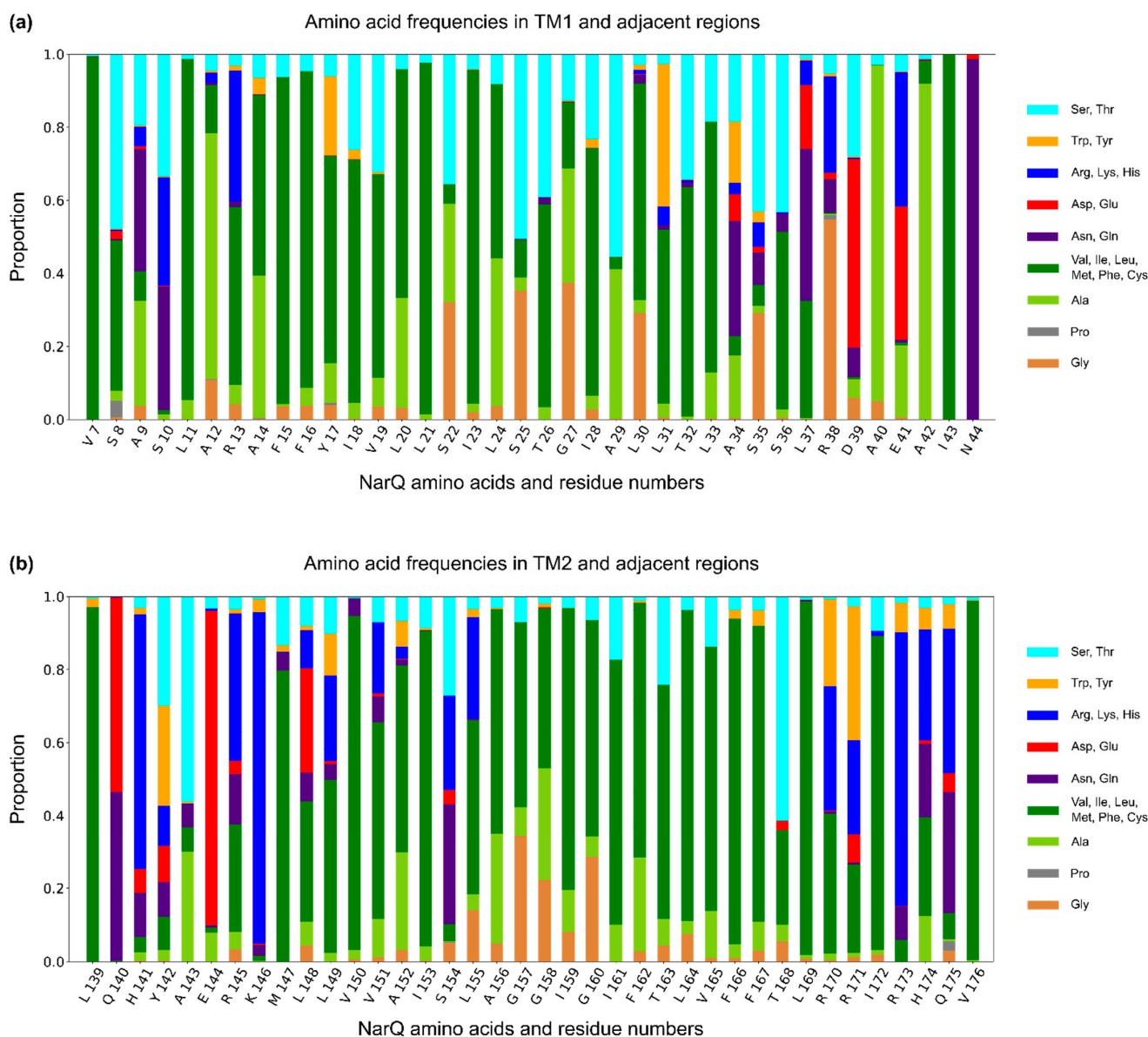


**Figure 9.** Amino acid frequencies at different TM1 (a) and TM2 (b) positions in multiple sequence alignment of NSHK genes. Amino acids with similar properties are grouped together for clarity. Patterned occurrences of glycine, serine, and threonine are evident.

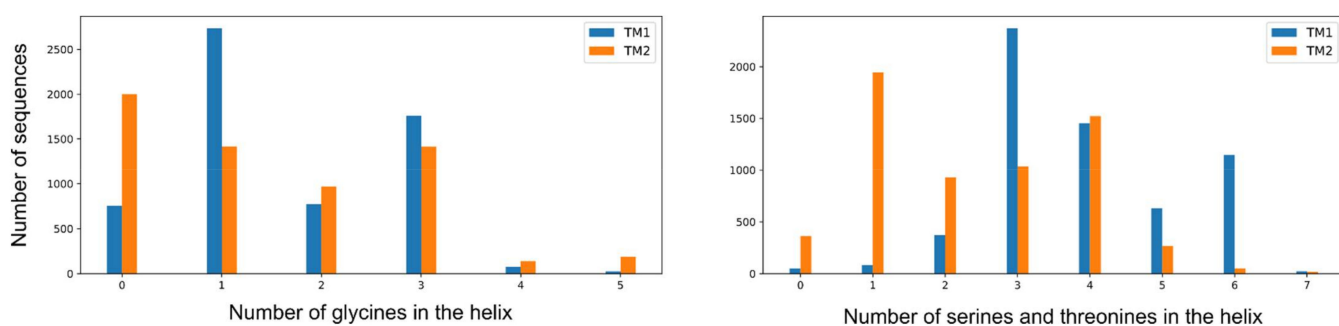


**Figure 10.** Abundance of glycines, serines, and threonines in transmembrane  $\alpha$ -helices in NSHKs. Each TM helix (TM1 and TM2) on average contains one to two glycines and three to four serines or threonines.

## 9. HAMP Domain of Nitrate- and Nitrite-Sensing Histidine Kinases

The HAMP domain is a previously enigmatic module often found in the cytoplasmic part of HKs, chemoreceptors, and sensory rhodopsin transducers adjacent to the TM domain [36,37,164]. Its main function is believed to be in converting the signal coming from the transmembrane domain to one that can be recognized by cytoplasmic domains such as DHp and CA. The first experimental structure of the HAMP domain, which was organized as a four-helical parallel coiled coil, was determined in 2006 [165], and more became available since that time [140,166–168], alongside with computational models for HAMP domains from other proteins [169–172] and supporting mutagenesis data [48,173–175].

Several mechanisms of HAMP domain signaling have been proposed, namely diagonal scissoring, helical rotation, and transitions between stable (compact) and dynamic states [25,35,37,176] as well as more complex three-state models [177,178]. X-ray structures of the sensor, TM, and HAMP domains of NarQ in ligand-free and ligand-bound forms provide one of the clearest pictures of signal transduction: piston-like shifts of the TM1 helices of the TM domain cause primarily scissoring in the HAMP, which leads to drastic changes in the distance between its C-terminal ends (Figure 11, [140]). Yet, due to the absence of full-length protein structures, for NarQ and other HKs, not all of the details of HAMP domain functioning are elucidated at the moment. The signal transduction mechanism may include different elements, and it may be different between different proteins [37].

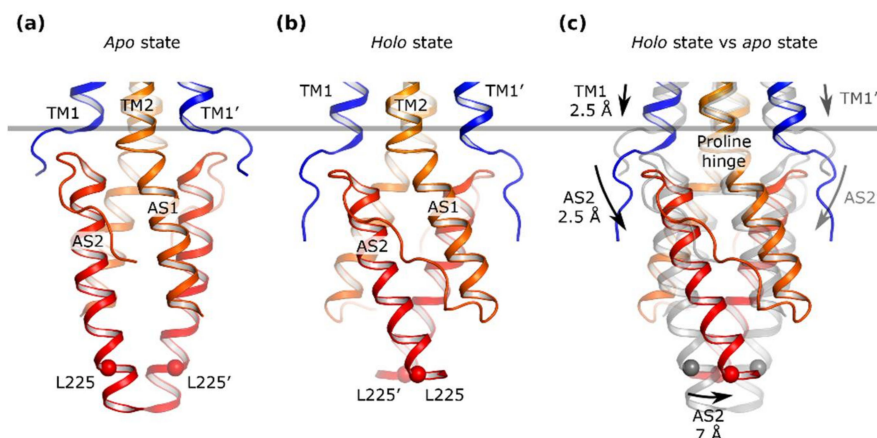


**Figure 11.** Details of the signal transduction from the TM domain to and through the HAMP domain. (a) Ligand-free state. (b) Ligand-bound state. (c) Superposition of the ligand-free (gray) and ligand-bound (colored) states. A piston-like displacement of the cytoplasmic end of the helix TM1 relative to TM2 and the TM2-AS1 proline hinge is transmitted to the membrane-proximal end of AS2 and results in lever-like rotations of the HAMP domain protomers around the hinges. Since the HAMP domain protomers move in opposite directions, the positions of membrane-distal ends of helices AS2 also change relative to each other. Positions of the Leu225 C $\alpha$  atom are marked with the spheres. The gray bar shows the position of TM1 ends in the apo state structure. The domains are aligned by the residues 175–177. Reproduced with permission from [140].

At the same time, *Bacteroidetes* NSHKs appear to lack HAMP domains altogether (Figure 5). There, the signal might be transduced from the TM domain to the DHp domain similarly to other HAMP-less HKs such as AgrC [179], BvgS [180,181], DesK [182], or DctB [183].

## 10. Signaling Helix Region of Nitrate- and Nitrite-Sensing Histidine Kinases

Many sensor HKs and adenylate and guanylate cyclases have a conserved  $\alpha$ -helical connector element between their domains dubbed signaling helix (S-helix), with the characteristic motif L-E-x-x-V-x-E-(R/K)-T-x-(E/D/Q)-L [184,185]. Since the proteins are usu-

ally homodimeric, the S-helix forms a parallel coiled coil. In addition to the S-helix, several other helical connectors that transmit signals have been identified in sensor proteins [169,179,182,186–188]. Whereas there is little doubt that the S-helix preserves helical conformation during signal transduction, experimental data on its structure are limited. The S-helix from *Sinorhizobium meliloti* DctB [183] was crystallized in a probably unphysiological antiparallel conformation (PDB ID 4GKG). Structures of Af1503 HAMP-EnvZ DHp/CA chimeras contain a submotif D-R-T [189,190]. While S-helices are usually preceded and followed by  $\alpha$ -helices in the flanking domains, they all seem to contain destabilizing elements (stutters and stammers [191,192]) that create tension and allow the protein to transition easily between different states [189,193,194].

The consensus motif of the respective region in proteobacterial NSHKs is L<sub>90</sub>-E<sub>83</sub>-Q<sub>20</sub>-R<sub>46</sub>-V<sub>83</sub>-A<sub>20</sub>-E<sub>45</sub>-K<sub>76</sub>-T<sub>86</sub>-A<sub>30</sub>-E<sub>18</sub>-L<sub>82</sub>, where the subscripts indicate the probability of observing the respective amino acid at this position (in percent). Modeling shows that there are two possible arrangements (Figure 12 [140]). Both are compatible with the structure of the HAMP domain in the ligand-free state but not in the ligand-bound state. Thus, it is likely that binding of the ligand leads to destabilization and/or dissociation of the S-helix residues [140]. We note that while *Bacteroidetes* NSHKs (Figures 2 and 5) probably have a continuous  $\alpha$ -helix connecting the TM helix with the PAS or DHp domain, the sequence of this connector helix is different from the canonical conserved sequence of S-helix [184,185].

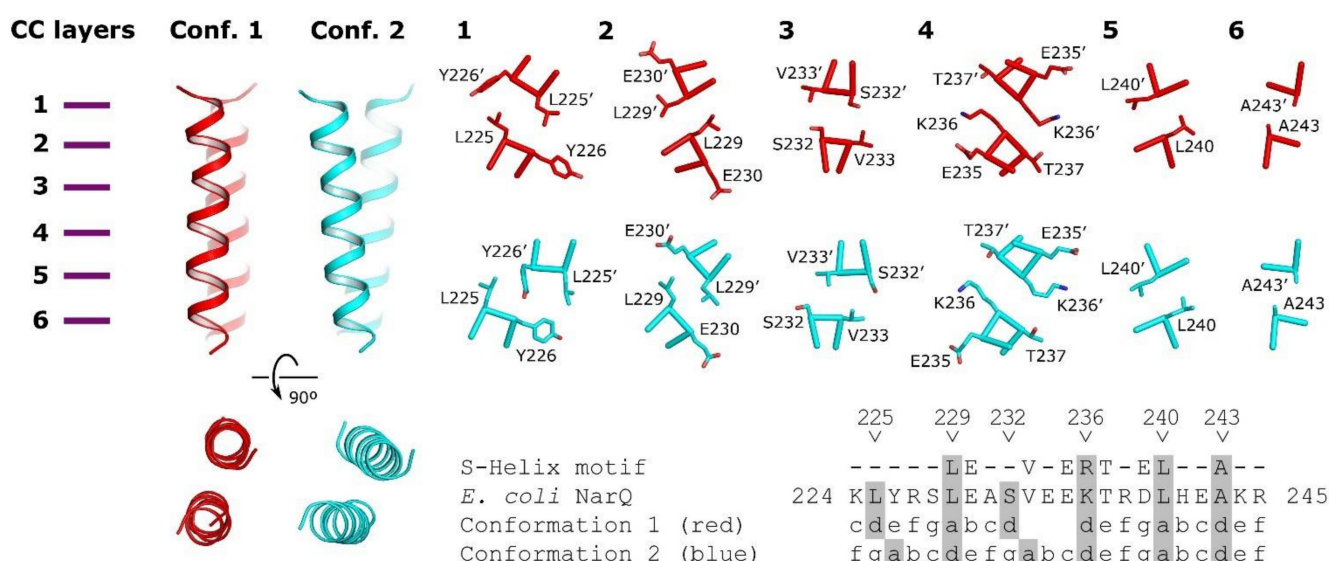


**Figure 12.** Coiled coil models of NarQ signaling helix domain. Two conformations are possible. Conformation 1 is shown in red and conformation 2 is shown in blue. The packing in layers 1–3 is different, while the packing in layers 4–6 is similar. The phase stutter is possible in the region of the residues 232–236. Residues Glu235, Lys236, and Thr237 belong to the characteristic conserved signaling helix motif (32). Reproduced with permission from [140].

## 11. GAF-Like Domain of Nitrate- and Nitrite-Sensing Histidine Kinases

The GAF domain is another conserved domain often found in sensory proteins [40]. GAFs usually consist of a five- or six-stranded antiparallel  $\beta$ -sheet and four or five  $\alpha$ -helices, and they dimerize in such a way that the N-terminal and C-terminal  $\alpha$ -helices form parallel coiled coils that are structurally congruent with other HK and TCS modules. In different proteins, GAFs bind cyclic nucleotides [195], bilins [196], heme [197,198], or Fe-S clusters [199]. The GAF domain of the free methionine-(R)-sulfoxide reductase from *Escherichia coli* has been shown to possess enzymatic activity [200].

Out of the 6121 NSHK genes that we found in the database InterPro [103], 582 were listed as having GAF domains, while in others, in particular in the *E. coli* NarQ and NarX, the respective region between S-helix and DHp is not recognized as GAF neither by Pfam [201] nor by InterPro [103]. Yet, the sequence is largely conserved, and we conclude

that all proteobacterial NSHKs have a GAF-like domain. The respective region is  $\approx 30$  amino acids shorter in the NarQ-like NSHKs from *Enterobacteriales*, *Pasteurellales*, *Vibrionales*, and *Alteromonadales*. Accordingly, homology modeling shows that NarQ-like NSHKs harbor a reduced GAF-like domain likely with only three  $\alpha$ -helices, whereas NarX-like NSHKs possess an almost complete GAF (Figure 13). Currently, no evidence is available that the NarQ or NarX GAF-like domain is able to independent sense intracellular signals; probably, it acts as a single transmitter. The absence of GAF-like domains in *Bacteroidetes* NSHKs underscores the assumption that the domain is not essential for the correct functioning of NSHKs.

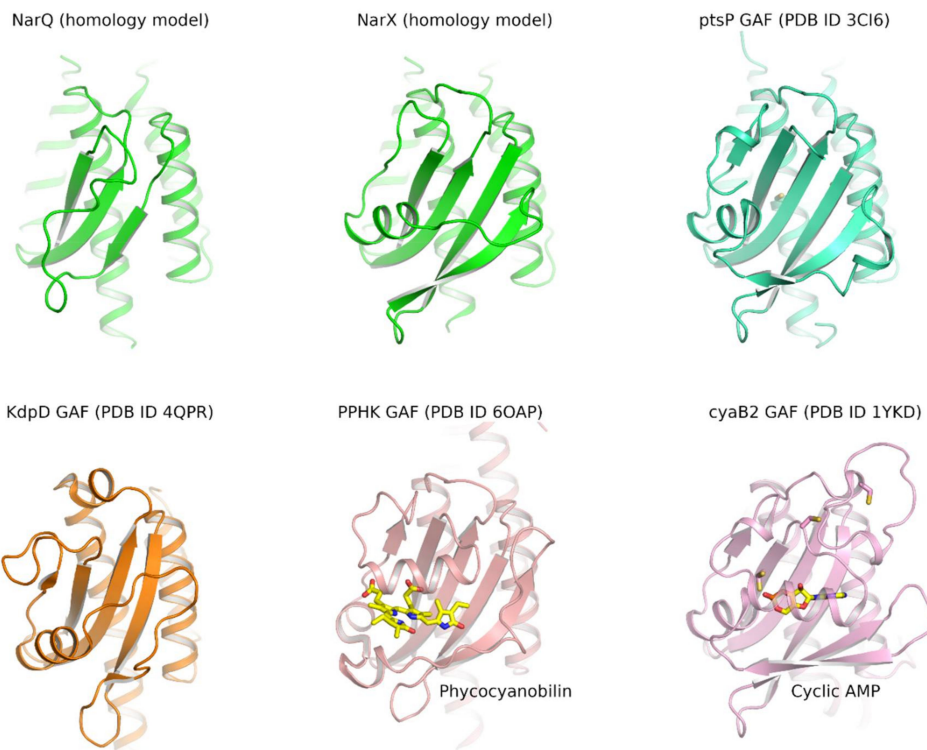


**Figure 13.** Structural models of different GAF domains: homology models of NarQ and NarX GAF-like domains, which are based on the structure of the *Acinetobacter baylyi* phosphoenolpyruvate-protein phosphotransferase (ptsP) GAF domain (PDB ID 3CI6); *E. coli* potassium sensor HK KdpD GAF domain (PDB ID 4QPR [202]); phycocyanobilin-bound *Leptolyngbya* sp. JSC-1 phosphorylation-responsive photosensitive histidine kinase (PPHK) GAF domain (PDB ID 6OAP, [203]); cyclic AMP-bound *Anabaena* adenylyl cyclase cyaB2 GAF domain (PDB ID 1YKD [204]). NarQ and NarX GAF-like domains are reduced in size compared to well-characterized GAF domains.

## 12. DHp Domain of Nitrate- and Nitrite-Sensing Histidine Kinases

DHp domains are essential domains of histidine kinases, playing several important roles. In the kinase state, the conserved histidine of the DHp domain acts as an acceptor of the phosphate from the catalytic domain; the phosphate is later transferred to the response regulator (or to the histidine phosphotransfer domain in hybrid histidine kinases). In the phosphatase state, the domain catalyzes dephosphorylation of the RR. DHp domains determine the specificity of HK:RR interactions [7,205–208].

Based on their sequences, DHp domains are grouped into several subfamilies [209]. All NSHK DHp domains belong to the HisKA\_3 subfamily; there, RR dephosphorylation is facilitated by a conserved D-x-x-x-Q motif adjacent to the conserved histidine [210,211] rather than by the E-x-x-x-T/N motif in the HisKA subfamily [212].

Many structures of DHp domains are currently available [23,25,41,58]. Generally, DHps are homodimers, where each protomer is formed by two antiparallel  $\alpha$ -helices. Depending on the loop in between, the two helices are arranged either clockwise or coun-

terclockwise within the DHp domain in different kinases; consequently, phosphorylation happens either in *trans* or in *cis* [213]. However, in NarQ and NarX, this general rule may not hold [214].

Whereas experimental structures of any NSHK DHp domain are not available at the moment, the structures of another member of the HisKA\_3 subfamily that have been determined previously can be used as a model. *Bacillus subtilis* DesK has been extensively characterized, and multiple X-ray structures in kinase and phosphatase states are available [208,215,216]; sequence identity of the DesK DHp domain to *E. coli* NarQ and NarX DHp domains is 29% and 26%, respectively. The regulation of DHp activity is achieved via the conformation of the first  $\alpha$ -helix and the conserved histidine, which are controlled by the preceding domain (the GAF-like domain in case of proteobacterial NSHKs) [208].

### 13. Catalytic Domain of Nitrate- and Nitrite-Sensing Histidine Kinases

Catalytic domains of histidine kinases catalyze transfer of the  $\gamma$ -phosphate group from ATP to the catalytic histidine of the DHp domain. They are a part of a larger protein superfamily comprising proteins similar to DNA gyrase B, topoisomerase, heat shock protein HSP90, phytochrome-like ATPases, and DNA mismatch repair proteins [217].

The activity of the catalytic domain is likely regulated not by itself but rather by the DHp domain, assuming a conformation that is more or less conducive to phosphorylation depending on the signaling state of the protein. Yet, there is another interesting possibility in some of the NSHKs. Opposite to the catalytic site, *E. coli* NarQ CA harbors two cysteine residues in close vicinity to each other, Cys455 and Cys494 (Figure 14). Cys455 is relatively well conserved among *Enterobacteriales* and *Pasteurellales* proteins; Cys494 is relatively well conserved among *Enterobacteriales* and *Vibrionales* proteins. In an unrelated HK SrrB, similar cysteines, Cys464 and Cys501, form an intramolecular disulfide bond, which responds to the cellular redox environment and affects autophosphorylation kinetics [218]. Thus, it is possible that the previously observed dependence of NarQ activity on aeration [219] is achieved via formation of the disulfide bond in the catalytic domain. Overall, the regulation of protein activity by redox-sensitive cysteines is a common phenomenon, also among TCSs such as ArcBA, PrrBA, RegBA [220,221], or the recently discovered AccSR [222].

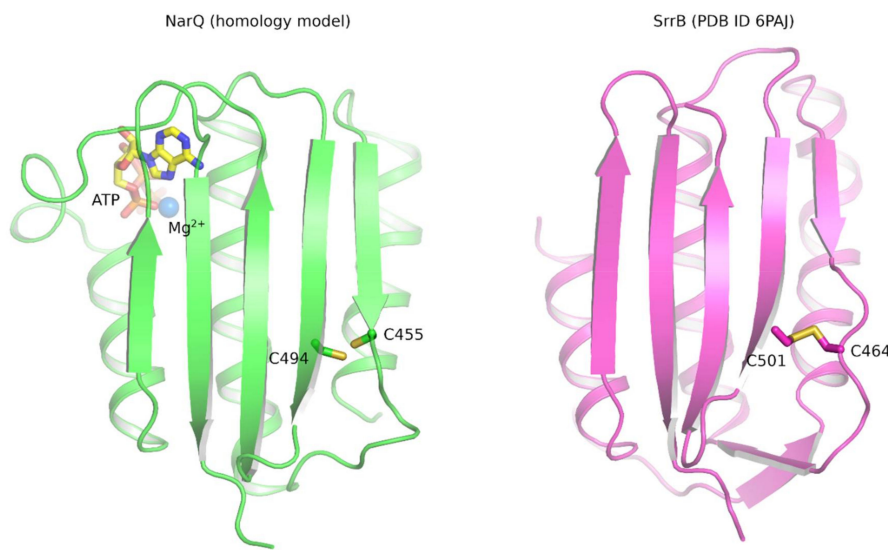


**Figure 14.** Structural models of NarQ (left, based on PDB IDs 3SL2 and 4GT8 [131,223]) and SrrB (right, PDB ID 6PAJ [218]) catalytic domains. The active site binds ATP and  $Mg^{2+}$  ion. In SrrB, Cys464 and Cys501 form an intramolecular disulfide bond, which responds to the cellular redox environment and affects autophosphorylation kinetics [218]. In NarQ, there is a conserved pair of similar cysteine residues, Cys455 and Cys494, that may also form a disulfide bond and react to the redox environment.

#### 14. Outlook

With this review, we attempted to summarize the knowledge about nitrate-responsive histidine kinases. It is apparent that they are important proteins for many microorganisms, and they have been studied accordingly. We know how and when they are activated and which cellular processes they regulate. Yet, many questions remain:

- What is the structure of full-length NSHKs in a native environment, in ligand-free and ligand-bound forms?
- How dynamic are full-length NSHKs? How many different conformations are assumed by NSHKs in each signaling state? How are these correlated with interactions with response regulator proteins?
- What is the mechanism of nitrate–nitrite discrimination by NSHKs at the molecular level? How does oxygen and/or the cellular redox environment affect the activity of NSHKs? Are there any other factors that affect the activity of NSHKs?
- What is the role of the GAF-like domains, and how is the signal transduced in GAF-less NSHKs from *Bacteroidetes*? How does the absence or presence of the HAMP domain influence signal transduction in NSHKs?
- What is the role of NSHKs in all the different organisms?

The information about the signaling mechanisms of NSHKs may be useful in the studies of other HKs as well and vice versa. The following questions go beyond the intricacies of nitrate regulation in microorganisms:

- How many different TCS sensors may be found in nature? What kind of signals and environmental factors may be recognized?
- Are the signal transduction mechanisms conserved between different HKs? Between HKs and chemoreceptors?
- What are the design principles of sensor HKs? How sensor HKs may be efficiently employed in the generation of new molecular biology tools, including artificial sensors [16–18] and reporters [15,22]?

Given the number of microorganisms and abundance of signaling systems in each of them, answering all of these questions will not be easy. However, it is clear that the advances in the available molecular biology techniques, and development of new ones, will bring deep insights into microbial signaling and its applications.

**Supplementary Materials:** The following are available online at <https://www.mdpi.com/article/10.3390/ijms22115933/s1>, Supplementary Dataset 1: Multiple sequence alignment of NSHKs in the FASTA format. Supplementary Dataset 2: Taxonomic annotation for the analyzed NSHK sequences. Supplementary Dataset 3: Data file for the phylogenetic tree depicted in Figures 2 and 4.

**Author Contributions:** Conceptualization, I.G.; Investigation, I.G. and V.A.A.; Writing—Original Draft Preparation, I.G. and V.A.A.; Writing—Review and Editing, I.G., V.A.A., P.O., I.M.G., V.V.N., O.S., A.R. and V.G. All authors have read and agreed to the published version of the manuscript.

**Funding:** This research was funded by the Russian Science Foundation, grant number 18-74-10053.

**Institutional Review Board Statement:** Not applicable.

**Informed Consent Statement:** Not applicable.

**Data Availability Statement:** Multiple sequence alignment, taxonomic annotation and phylogenetic tree for the analyzed NSHK sequences are available as Supplementary Materials.

**Conflicts of Interest:** The authors declare no conflict of interest. The funders had no role in the design of the study; in the collection, analyses, or interpretation of data; in the writing of the manuscript, or in the decision to publish the results.

## References

1. Galperin, M.Y. A census of membrane-bound and intracellular signal transduction proteins in bacteria: Bacterial IQ, extroverts and introverts. *BMC Microbiol.* **2005**, *5*, 35. [[CrossRef](#)] [[PubMed](#)]
2. Wuichet, K.; Cantwell, B.J.; Zhulin, I.B. Evolution and phyletic distribution of two-component signal transduction systems. *Curr. Opin. Microbiol.* **2010**, *13*, 219–225. [[CrossRef](#)]
3. Capra, E.J.; Laub, M.T. Evolution of Two-Component Signal Transduction Systems. *Annu. Rev. Microbiol.* **2012**, *66*, 325–347. [[CrossRef](#)] [[PubMed](#)]
4. Wassenaar, T.M.; Wanchai, V.; Alkam, D.; Nookae, I.; Ussery, D.W. Conservation of two-component signal transduction systems in *E. coli*, *Salmonella*, and Across 100,000 bacteria of various bacterial Phyla. In *Molecular Mechanisms of Microbial Evolution; Grand Challenges in Biology and Biotechnology*; Rampelotto, P.H., Ed.; Springer International Publishing: Cham, Switzerland, 2018; pp. 153–174, ISBN 978-3-319-69078-0.
5. Galperin, M.Y.; Makarova, K.S.; Wolf, Y.I.; Koonin, E.V. Phylogenetic Distribution and Lineage-Specific Domain Architectures of Archaeal Two-Component Signal Transduction Systems. *J. Bacteriol.* **2017**, *200*. [[CrossRef](#)]
6. Yamamoto, K.; Hirao, K.; Oshima, T.; Aiba, H.; Utsumi, R.; Ishihama, A. Functional Characterization In Vitro of All Two-component Signal Transduction Systems from *Escherichia coli*. *J. Biol. Chem.* **2005**, *280*, 1448–1456. [[CrossRef](#)] [[PubMed](#)]
7. Podgornaia, A.I.; Laub, M.T. Determinants of specificity in two-component signal transduction. *Curr. Opin. Microbiol.* **2013**, *16*, 156–162. [[CrossRef](#)] [[PubMed](#)]
8. Krell, T.; Lacal, J.; Busch, A.; Silva-Jiménez, H.; Guazzaroni, M.-E.; Ramos, J.L. Bacterial Sensor Kinases: Diversity in the Recognition of Environmental Signals. *Annu. Rev. Microbiol.* **2010**, *64*, 539–559. [[CrossRef](#)]
9. Schramke, H.; Wang, Y.; Heermann, R.; Jung, K. Stimulus perception by histidine kinases. In *Stress and Environmental Regulation of Gene Expression and Adaptation in Bacteria*; Wiley: Hoboken, NJ, USA, 2016; pp. 282–300.
10. Ortega, Á.; Zhulin, I.B.; Krell, T. Sensory Repertoire of Bacterial Chemoreceptors. *Microbiol. Mol. Biol. Rev.* **2017**, *81*, e00033-17. [[CrossRef](#)]
11. Gumerov, V.M.; Andrianova, E.P.; Zhulin, I.B. Diversity of bacterial chemosensory systems. *Curr. Opin. Microbiol.* **2021**, *61*, 42–50. [[CrossRef](#)]
12. LaSarre, B.; Federle, M.J. Exploiting Quorum Sensing to Confuse Bacterial Pathogens. *Microbiol. Mol. Biol. Rev.* **2013**, *77*, 73–111. [[CrossRef](#)]
13. Bem, A.E.; Velikova, N.; Pellicer, M.T.; van Baarlen, P.; Marina, A.; Wells, J.M. Bacterial Histidine Kinases as Novel Antibacterial Drug Targets. *ACS Chem. Biol.* **2015**, *10*, 213–224. [[CrossRef](#)] [[PubMed](#)]
14. Rajput, A.; Seif, Y.; Choudhary, K.S.; Dalldorf, C.; Poudel, S.; Monk, J.M.; Palsson, B.O. Pangenome Analytics Reveal Two-Component Systems as Conserved Targets in ESKAPE Pathogens. *mSystems* **2021**, *6*. [[CrossRef](#)] [[PubMed](#)]
15. Nasu, Y.; Shen, Y.; Kramer, L.; Campbell, R.E. Structure- and mechanism-guided design of single fluorescent protein-based biosensors. *Nat. Chem. Biol.* **2021**, *17*, 509–518. [[CrossRef](#)] [[PubMed](#)]
16. Hansen, J.; Mailand, E.; Swaminathan, K.K.; Schreiber, J.; Angelici, B.; Benenson, Y. Transplantation of prokaryotic two-component signaling pathways into mammalian cells. *Proc. Natl. Acad. Sci. USA* **2014**, *111*, 15705–15710. [[CrossRef](#)]
17. Kowallis, K.A.; Duvall, S.W.; Zhao, W.; Childers, W.S. Manipulation of bacterial signaling using engineered Histidine Kinases. In *Methods in Molecular Biology*; Evers, C.E., Ed.; Springer US: New York, NY, USA, 2020; pp. 141–163, ISBN 978-1-4939-9884-5.
18. Scheller, L.; Schmollack, M.; Bertschi, A.; Mansouri, M.; Saxena, P.; Fussenegger, M. Phosphoregulated orthogonal signal transduction in mammalian cells. *Nat. Commun.* **2020**, *11*, 1–10. [[CrossRef](#)] [[PubMed](#)]
19. Mazé, A.; Benenson, Y. Artificial signaling in mammalian cells enabled by prokaryotic two-component system. *Nat. Chem. Biol.* **2019**, *16*, 179–187. [[CrossRef](#)]
20. Jung, K.; Fabiani, F.; Hoyer, E.; Lassak, J. Bacterial transmembrane signalling systems and their engineering for biosensing. *Open Biol.* **2018**, *8*, 180023. [[CrossRef](#)] [[PubMed](#)]
21. Woo, S.-G.; Moon, S.-J.; Kim, S.K.; Kim, T.H.; Lim, H.S.; Yeon, G.-H.; Sung, B.H.; Lee, C.-H.; Lee, S.-G.; Hwang, J.H.; et al. A designed whole-cell biosensor for live diagnosis of gut inflammation through nitrate sensing. *Biosens. Bioelectron.* **2020**, *168*, 112523. [[CrossRef](#)]
22. Tanna, T.; Ramachanderan, R.; Platt, R.J. Engineered bacteria to report gut function: Technologies and implementation. *Curr. Opin. Microbiol.* **2021**, *59*, 24–33. [[CrossRef](#)] [[PubMed](#)]
23. Zschiedrich, C.P.; Keidel, V.; Szurmant, H. Molecular Mechanisms of Two-Component Signal Transduction. *J. Mol. Biol.* **2016**, *428*, 3752–3775. [[CrossRef](#)]
24. Gao, R.; Bouillet, S.; Stock, A.M. Structural Basis of Response Regulator Function. *Annu. Rev. Microbiol.* **2019**, *73*, 175–197. [[CrossRef](#)] [[PubMed](#)]
25. Bhate, M.P.; Molnar, K.S.; Goulian, M.; DeGrado, W.F. Signal Transduction in Histidine Kinases: Insights from New Structures. *Structure* **2015**, *23*, 981–994. [[CrossRef](#)] [[PubMed](#)]
26. Galperin, M.Y. Diversity of structure and function of response regulator output domains. *Curr. Opin. Microbiol.* **2010**, *13*, 150–159. [[CrossRef](#)] [[PubMed](#)]
27. Parkinson, J.S.; Hazelbauer, G.L.; Falke, J.J. Signaling and sensory adaptation in *Escherichia coli* chemoreceptors: 2015 update. *Trends Microbiol.* **2015**, *23*, 257–266. [[CrossRef](#)]
28. Bi, S.; Sourjik, V. Stimulus sensing and signal processing in bacterial chemotaxis. *Curr. Opin. Microbiol.* **2018**, *45*, 22–29. [[CrossRef](#)]

29. Yang, W.; Briegel, A. Diversity of Bacterial Chemosensory Arrays. *Trends Microbiol.* **2020**, *28*, 68–80. [[CrossRef](#)] [[PubMed](#)]
30. Muok, A.R.; Briegel, A.; Crane, B.R. Regulation of the chemotaxis histidine kinase CheA: A structural perspective. *Biochim. Biophys. Acta Biomembr.* **2020**, *1862*, 183030. [[CrossRef](#)]
31. Briegel, A.; Ladinsky, M.S.; Oikonomou, C.; Jones, C.W.; Harris, M.J.; Fowler, D.J.; Chang, Y.-W.; Thompson, L.K.; Armitage, J.P.; Jensen, G.J. Structure of bacterial cytoplasmic chemoreceptor arrays and implications for chemotactic signaling. *eLife* **2014**, *3*, e02151. [[CrossRef](#)]
32. Möglich, A. Signal transduction in photoreceptor histidine kinases. *Protein Sci.* **2019**, *28*, 1923–1946. [[CrossRef](#)]
33. Gumerov, V.M.; Ortega, D.R.; Adebali, O.; Ulrich, L.E.; Zhulin, I.B. MiST 3.0: An updated microbial signal transduction database with an emphasis on chemosensory systems. *Nucleic Acids Res.* **2020**, *48*, D459–D464. [[CrossRef](#)]
34. Galperin, M.Y.; Nikolskaya, A.N.; Koonin, E.V. Novel domains of the prokaryotic two-component signal transduction systems. *FEMS Microbiol. Lett.* **2001**, *203*, 11–21. [[CrossRef](#)] [[PubMed](#)]
35. Parkinson, J.S. Signaling Mechanisms of HAMP Domains in Chemoreceptors and Sensor Kinases. *Annu. Rev. Microbiol.* **2010**, *64*, 101–122. [[CrossRef](#)] [[PubMed](#)]
36. Dunin-Horkawicz, S.; Lupas, A.N. Comprehensive Analysis of HAMP Domains: Implications for Transmembrane Signal Transduction. *J. Mol. Biol.* **2010**, *397*, 1156–1174. [[CrossRef](#)] [[PubMed](#)]
37. Gushchin, I.; Gordeliy, V. Transmembrane Signal Transduction in Two-Component Systems: Piston, Scissoring, or Helical Rotation? *BioEssays* **2018**, *40*, 1700197. [[CrossRef](#)]
38. Möglich, A.; Ayers, R.A.; Moffat, K. Structure and Signaling Mechanism of Per-ARNT-Sim Domains. *Structure* **2009**, *17*, 1282–1294. [[CrossRef](#)]
39. Stuffle, E.C.; Johnson, M.S.; Watts, K.J. PAS domains in bacterial signal transduction. *Curr. Opin. Microbiol.* **2021**, *61*, 8–15. [[CrossRef](#)]
40. Aravind, L.; Ponting, C.P. The GAF domain: An evolutionary link between diverse phototransducing proteins. *Trends Biochem. Sci.* **1997**, *22*, 458–459. [[CrossRef](#)]
41. Jacob-Dubuisson, F.; Mechaly, A.; Betton, J.-M.; Antoine, R. Structural insights into the signalling mechanisms of two-component systems. *Nat. Rev. Genet.* **2018**, *16*, 585–593. [[CrossRef](#)]
42. Cheung, J.; Hendrickson, W.A. Sensor domains of two-component regulatory systems. *Curr. Opin. Microbiol.* **2010**, *13*, 116–123. [[CrossRef](#)]
43. Upadhyay, A.; Fleetwood, A.D.; Adebali, O.; Finn, R.; Zhulin, I.B. Cache Domains That are Homologous to, but Different from PAS Domains Comprise the Largest Superfamily of Extracellular Sensors in Prokaryotes. *PLoS Comput. Biol.* **2016**, *12*, e1004862. [[CrossRef](#)] [[PubMed](#)]
44. Krikos, A.; Conley, M.P.; Boyd, A.; Berg, H.C.; Simon, M.I. Chimeric chemosensory transducers of *Escherichia coli*. *Proc. Natl. Acad. Sci. USA* **1985**, *82*, 1326–1330. [[CrossRef](#)] [[PubMed](#)]
45. Utsumi, R.; Brissette, R.; Rampersaud, A.; Forst, S.; Oosawa, K.; Inouye, M. Activation of bacterial porin gene expression by a chimeric signal transducer in response to aspartate. *Science* **1989**, *245*, 1246–1249. [[CrossRef](#)] [[PubMed](#)]
46. Baumgartner, J.W.; Kim, C.; Brissette, R.E.; Inouye, M.; Park, C.; Hazelbauer, G.L. Transmembrane signalling by a hybrid protein: Communication from the domain of chemoreceptor Trg that recognizes sugar-binding proteins to the kinase/phosphatase domain of osmosensor EnvZ. *J. Bacteriol.* **1994**, *176*, 1157–1163. [[CrossRef](#)] [[PubMed](#)]
47. Ward, S.M.; Delgado, A.; Gunsalus, R.P.; Manson, M.D. A NarX-Tar chimera mediates repellent chemotaxis to nitrate and nitrite. *Mol. Microbiol.* **2002**, *44*, 709–719. [[CrossRef](#)] [[PubMed](#)]
48. Appleman, J.A.; Chen, L.-L.; Stewart, V. Probing Conservation of HAMP Linker Structure and Signal Transduction Mechanism through Analysis of Hybrid Sensor Kinases. *J. Bacteriol.* **2003**, *185*, 4872–4882. [[CrossRef](#)]
49. Ward, S.M.; Bormans, A.F.; Manson, M.D. Mutationally Altered Signal Output in the Nart (NarX-Tar) Hybrid Chemoreceptor. *J. Bacteriol.* **2006**, *188*, 3944–3951. [[CrossRef](#)]
50. Bi, S.; Pollard, A.M.; Yang, Y.; Jin, F.; Sourjik, V. Engineering Hybrid Chemotaxis Receptors in Bacteria. *ACS Synth. Biol.* **2016**, *5*, 989–1001. [[CrossRef](#)]
51. Lehning, C.E.; Heidelberger, J.B.; Reinhard, J.; Nørholm, M.; Draheim, R.R. A Modular High-Throughput In Vivo Screening Platform Based on Chimeric Bacterial Receptors. *ACS Synth. Biol.* **2017**, *6*, 1315–1326. [[CrossRef](#)]
52. Luu, R.A.; Schomer, R.A.; Brunton, C.N.; Truong, R.; Ta, A.P.; Tan, W.A.; Parales, J.V.; Wang, Y.-J.; Huo, Y.-W.; Liu, S.-J.; et al. Hybrid Two-Component Sensors for Identification of Bacterial Chemoreceptor Function. *Appl. Environ. Microbiol.* **2019**, *85*, 85. [[CrossRef](#)]
53. Pineda-Molina, E.; Reyes-Darias, J.-A.; Lacal, J.; Ramos, J.L.; García-Ruiz, J.M.; Gavira, J.A.; Krell, T. Evidence for chemoreceptors with bimodular ligand-binding regions harboring two signal-binding sites. *Proc. Natl. Acad. Sci. USA* **2012**, *109*, 18926–18931. [[CrossRef](#)]
54. Gavira, J.A.; Matilla, M.A.; Fernández, M.; Krell, T. The structural basis for signal promiscuity in a bacterial chemoreceptor. *FEBS J.* **2021**, *288*, 2294–2310. [[CrossRef](#)] [[PubMed](#)]
55. Monk, I.R.; Shaikh, N.; Begg, S.L.; Gajdiss, M.; Sharkey, L.K.R.; Lee, J.Y.H.; Pidot, S.J.; Seemann, T.; Kuiper, M.; Winnen, B.; et al. Zinc-binding to the cytoplasmic PAS domain regulates the essential WalK histidine kinase of *Staphylococcus aureus*. *Nat. Commun.* **2019**, *10*, 1–13. [[CrossRef](#)] [[PubMed](#)]

56. Sobran, M.A.; Cotter, P.A. The BvgS PAS Domain, an Independent Sensory Perception Module in the *Bordetella bronchiseptica* BvgAS Phosphorelay. *J. Bacteriol.* **2019**, *201*. [[CrossRef](#)] [[PubMed](#)]
57. Willett, J.W.; Crosson, S. Atypical modes of bacterial histidine kinase signaling. *Mol. Microbiol.* **2016**, *103*, 197–202. [[CrossRef](#)]
58. Buschiazzo, A.; Trajtenberg, F. Two-Component Sensing and Regulation: How Do Histidine Kinases Talk with Response Regulators at the Molecular Level? *Annu. Rev. Microbiol.* **2019**, *73*, 507–528. [[CrossRef](#)] [[PubMed](#)]
59. Clark, I.C.; Mensa, B.; Ochs, C.J.; Schmidt, N.W.; Mravic, M.; Quintana, F.J.; DeGrado, W.F.; Abate, A.R. Protein design-scapes generated by microfluidic DNA assembly elucidate domain coupling in the bacterial histidine kinase CpxA. *Proc. Natl. Acad. Sci. USA* **2021**, *118*. [[CrossRef](#)]
60. Kraft, B.; Strous, M.; Tegetmeyer, H.E. Microbial nitrate respiration—Genes, enzymes and environmental distribution. *J. Biotechnol.* **2011**, *155*, 104–117. [[CrossRef](#)] [[PubMed](#)]
61. Kracke, F.; Vassilev, I.; Krömer, J.O. Microbial electron transport and energy conservation—The foundation for optimizing bioelectrochemical systems. *Front. Microbiol.* **2015**, *6*, 575. [[CrossRef](#)]
62. Kuypers, M.M.M.; Marchant, H.; Kartal, B. The microbial nitrogen-cycling network. *Nat. Rev. Genet.* **2018**, *16*, 263–276. [[CrossRef](#)]
63. Hallin, S.; Philippot, L.; Löfller, F.E.; Sanford, R.A.; Jones, C. Genomics and Ecology of Novel N<sub>2</sub>O-Reducing Microorganisms. *Trends Microbiol.* **2018**, *26*, 43–55. [[CrossRef](#)]
64. Uden, G.; Klein, R. Sensing of O<sub>2</sub> and nitrate by bacteria: Alternative strategies for transcriptional regulation of nitrate respiration by O<sub>2</sub> and nitrate. *Environ. Microbiol.* **2021**, *23*, 5–14. [[CrossRef](#)] [[PubMed](#)]
65. Ravishankara, A.R.; Daniel, J.S.; Portmann, R. Nitrous Oxide (N<sub>2</sub>O): The Dominant Ozone-Depleting Substance Emitted in the 21st Century. *Science* **2009**, *326*, 123–125. [[CrossRef](#)] [[PubMed](#)]
66. Jones, S.A.; Chowdhury, F.Z.; Fabich, A.J.; Anderson, A.; Schreiner, D.M.; House, A.L.; Autieri, S.M.; Leatham, M.P.; Lins, J.J.; Jorgensen, M.; et al. Respiration of *Escherichia coli* in the Mouse Intestine. *Infect. Immun.* **2007**, *75*, 4891–4899. [[CrossRef](#)] [[PubMed](#)]
67. Jones, S.A.; Gibson, T.; Maltby, R.C.; Chowdhury, F.Z.; Stewart, V.; Cohen, P.S.; Conway, T. Anaerobic Respiration of *Escherichia coli* in the Mouse Intestine. *Infect. Immun.* **2011**, *79*, 4218–4226. [[CrossRef](#)]
68. Winter, S.E.; Winter, M.G.; Xavier, M.N.; Thiennimitr, P.; Poon, V.; Keestra, A.M.; Laughlin, R.C.; Gomez, G.; Wu, J.; Lawhon, S.D.; et al. Host-derived nitrate boosts growth of *E. coli* in the inflamed gut. *Science* **2013**, *339*, 708–711. [[CrossRef](#)]
69. Koch, C.; Gladwin, M.T.; Freeman, B.A.; Lundberg, J.O.; Weitzberg, E.; Morris, A. Enterosalivary nitrate metabolism and the microbiome: Intersection of microbial metabolism, nitric oxide and diet in cardiac and pulmonary vascular health. *Free Radic. Biol. Med.* **2017**, *105*, 48–67. [[CrossRef](#)]
70. Graf, J.S.; Schorn, S.; Kitzinger, K.; Ahmerkamp, S.; Woehle, C.; Huettel, B.; Schubert, C.J.; Kuypers, M.M.M.; Milucka, J. Anaerobic endosymbiont generates energy for ciliate host by denitrification. *Nat. Cell Biol.* **2021**, *591*, 445–450. [[CrossRef](#)]
71. Stewart, V. Nitrate- and nitrite-responsive sensors NarX and NarQ of proteobacteria. *Biochem. Soc. Trans.* **2003**, *31*, 1–10. [[CrossRef](#)]
72. Malhotra, V.; Agrawal, R.; Duncan, T.R.; Saini, D.K.; Clark-Curtiss, J.E. Mycobacterium tuberculosis Response Regulators, DevR and NarL, Interact In Vivo and Co-regulate Gene Expression during Aerobic Nitrate Metabolism. *J. Biol. Chem.* **2015**, *290*, 8294–8309. [[CrossRef](#)]
73. Niemann, V.; Koch-Singenstreue, M.; Neu, A.; Nilkens, S.; Götz, F.; Uden, G.; Stehle, T. The NreA Protein Functions as a Nitrate Receptor in the Staphylococcal Nitrate Regulation System. *J. Mol. Biol.* **2014**, *426*, 1539–1553. [[CrossRef](#)]
74. Martín-Mora, D.; Ortega, Á.; Matilla, M.A.; Martínez-Rodríguez, S.; Gavira, J.A.; Krell, T. The Molecular Mechanism of Nitrate Chemotaxis via Direct Ligand Binding to the PilJ Domain of McpN. *mBio* **2019**, *10*, e02334-18. [[CrossRef](#)]
75. Boudes, M.; Lazar, N.; Graille, M.; Durand, D.; Gaidenko, T.A.; Stewart, V.; Van Tilburgh, H. The structure of the NasR transcription antiterminator reveals a one-component system with a NIT nitrate receptor coupled to an ANTAR RNA-binding effector. *Mol. Microbiol.* **2012**, *85*, 431–444. [[CrossRef](#)] [[PubMed](#)]
76. Shu, C.J.; Ulrich, L.E.; Zhulin, I.B. The NIT domain: A predicted nitrate-responsive module in bacterial sensory receptors. *Trends Biochem. Sci.* **2003**, *28*, 121–124. [[CrossRef](#)]
77. Shu, C.J.; Zhulin, I.B. ANTAR: An RNA-binding domain in transcription antitermination regulatory proteins. *Trends Biochem. Sci.* **2002**, *27*, 3–5. [[CrossRef](#)]
78. Gushchin, I.; Melnikov, I.; Polovinkin, V.; Ishchenko, A.; Gordeliy, V. Crystal Structure of a Proteolytic Fragment of the Sensor Histidine Kinase NarQ. *Crystals* **2020**, *10*, 149. [[CrossRef](#)]
79. Stewart, V.; MacGregor, C.H. Nitrate reductase in *Escherichia coli* K-12: Involvement of chlC, chlE, and chlG loci. *J. Bacteriol.* **1982**, *151*, 788–799. [[CrossRef](#)] [[PubMed](#)]
80. Stewart, V. Requirement of Fnr and NarL functions for nitrate reductase expression in *Escherichia coli* K-12. *J. Bacteriol.* **1982**, *151*, 1320–1325. [[CrossRef](#)] [[PubMed](#)]
81. Iuchi, S.; Lin, E.C. The narL gene product activates the nitrate reductase operon and represses the fumarate reductase and trimethylamine N-oxide reductase operons in *Escherichia coli*. *Proc. Natl. Acad. Sci. USA* **1987**, *84*, 3901–3905. [[CrossRef](#)]
82. Stewart, V.; Parales, J. Identification and expression of genes narL and narX of the nar (nitrate reductase) locus in *Escherichia coli* K-12. *J. Bacteriol.* **1988**, *170*, 1589–1597. [[CrossRef](#)]
83. Stewart, V.; Parales, J.; Merkel, S.M. Structure of genes narL and narX of the nar (nitrate reductase) locus in *Escherichia coli* K-12. *J. Bacteriol.* **1989**, *171*, 2229–2234. [[CrossRef](#)]

84. Nohno, T.; Noji, S.; Taniguchi, S.; Saito, T. ThenarXandnarL genes encoding the nitrate-sensing regulators of *Escherichia coli* are homologous to a family of prokaryotic two-component regulatory genes. *Nucleic Acids Res.* **1989**, *17*, 2947–2957. [CrossRef]
85. Chiang, R.C.; Cavicchioli, R.; Gunsalus, R.P. Identification and characterization of narQ, a second nitrate sensor for nitrate-dependent gene regulation in *Escherichia coli*. *Mol. Microbiol.* **1992**, *6*, 1913–1923. [CrossRef] [PubMed]
86. Rabin, R.S.; Stewart, V. Either of two functionally redundant sensor proteins, NarX and NarQ, is sufficient for nitrate regulation in *Escherichia coli* K-12. *Proc. Natl. Acad. Sci. USA* **1992**, *89*, 8419–8423. [CrossRef]
87. Rabin, R.S.; Stewart, V. Dual response regulators (NarL and NarP) interact with dual sensors (NarX and NarQ) to control nitrate- and nitrite-regulated gene expression in *Escherichia coli* K-12. *J. Bacteriol.* **1993**, *175*, 3259–3268. [CrossRef]
88. Noriega, C.E.; Lin, H.-Y.; Chen, L.-L.; Williams, S.B.; Stewart, V. Asymmetric cross-regulation between the nitrate-responsive NarX-NarL and NarQ-NarP two-component regulatory systems from *Escherichia coli* K-12. *Mol. Microbiol.* **2010**, *75*, 394–412. [CrossRef]
89. Constantinidou, C.; Hobman, J.L.; Griffiths, L.; Patel, M.D.; Penn, C.W.; Cole, J.A.; Overton, T.W. A Reassessment of the FNR Regulon and Transcriptomic Analysis of the Effects of Nitrate, Nitrite, NarXL, and NarQP as *Escherichia coli* K12 Adapts from Aerobic to Anaerobic Growth. *J. Biol. Chem.* **2006**, *281*, 4802–4815. [CrossRef]
90. Fleischmann, R.D.; Adams, M.D.; White, O.; Clayton, R.A.; Kirkness, E.F.; Kerlavage, A.R.; Bult, C.J.; Tomb, J.F.; Dougherty, B.A.; Merrick, J.M.; et al. Whole-genome random sequencing and assembly of *Haemophilus influenzae* Rd. *Science* **1995**, *269*, 496–512. [CrossRef] [PubMed]
91. Härtig, E.; Schiek, U.; Vollack, K.-U.; Zumft, W.G. Nitrate and Nitrite Control of Respiratory Nitrate Reduction in Denitrifying *Pseudomonas stutzeri* by a Two-Component Regulatory System Homologous to NarXL of *Escherichia coli*. *J. Bacteriol.* **1999**, *181*, 3658–3665. [CrossRef]
92. Schreiber, K.; Krieger, R.; Benkert, B.; Eschbach, M.; Arai, H.; Schobert, M.; Jahn, D. The Anaerobic Regulatory Network Required for *Pseudomonas aeruginosa* Nitrate Respiration. *J. Bacteriol.* **2007**, *189*, 4310–4314. [CrossRef] [PubMed]
93. Van Alst, N.E.; Picardo, K.F.; Iglesias, B.H.; Haidaris, C.G. Nitrate Sensing and Metabolism Modulate Motility, Biofilm Formation, and Virulence in *Pseudomonas aeruginosa*. *Infect. Immun.* **2007**, *75*, 3780–3790. [CrossRef] [PubMed]
94. Lissenden, S.; Mohan, S.; Overton, T.; Regan, T.; Crooke, H.; Cardinale, J.A.; Householder, T.C.; Adams, P.; O’Conner, C.D.; Clark, V.L.; et al. Identification of transcription activators that regulate gonococcal adaptation from aerobic to anaerobic or oxygen-limited growth. *Mol. Microbiol.* **2000**, *37*, 839–855. [CrossRef]
95. Whitehead, R.N.; Overton, T.W.; Snyder, L.A.S.; McGowan, S.J.; Smith, H.; Cole, J.A.; Saunders, N.J. The small FNR regulon of *Neisseria gonorrhoeae*: Comparison with the larger *Escherichia coli* FNR regulon and interaction with the NarQ-NarP regulon. *BMC Genom.* **2007**, *8*, 35. [CrossRef] [PubMed]
96. Dong, Y.; Wang, J.; Fu, H.; Zhou, G.; Shi, M.; Gao, H. A Crp-Dependent Two-Component System Regulates Nitrate and Nitrite Respiration in *Shewanella oneidensis*. *PLoS ONE* **2012**, *7*, e51643. [CrossRef]
97. Gupta, A.; Bedre, R.; Thapa, S.S.; Sabrin, A.; Wang, G.; Dassanayake, M.; Grove, A. Global Awakening of Cryptic Biosynthetic Gene Clusters in *Burkholderia thailandensis*. *ACS Chem. Biol.* **2017**, *12*, 3012–3021. [CrossRef]
98. Mangalea, M.R.; Borlee, B.R. The NarX-NarL Two-Component System Is a Global Regulator of Biofilm Formation, Natural Product Biosynthesis, and Host-Associated Survival in *Burkholderia Pseudomallei*. *bioRxiv* **2020**. [CrossRef]
99. Land, M.; Hauser, L.; Jun, S.-R.; Nookaew, I.; Leuze, M.R.; Ahn, T.-H.; Karpinets, T.; Lund, O.; Kora, G.; Wassenaar, T.; et al. Insights from 20 years of bacterial genome sequencing. *Funct. Integr. Genom.* **2015**, *15*, 141–161. [CrossRef]
100. Franzosa, E.A.; Hsu, T.; Sirota-Madi, A.; Shafquat, A.; Abu-Ali, G.; Morgan, X.C.; Huttenhower, C. Sequencing and beyond: Integrating molecular ‘omics’ for microbial community profiling. *Nat. Rev. Genet.* **2015**, *13*, 360–372. [CrossRef] [PubMed]
101. Sayers, E.W.; Cavanaugh, M.; Clark, K.; Pruitt, K.D.; Schoch, C.L.; Sherry, S.T.; Karsch-Mizrachi, I. GenBank. *Nucleic Acids Res.* **2021**, *49*, D92–D96. [CrossRef] [PubMed]
102. The UniProt Consortium. UniProt: The universal protein knowledgebase in 2021. *Nucleic Acids Res.* **2021**, *49*, D480–D489. [CrossRef] [PubMed]
103. Blum, M.; Chang, H.-Y.; Chuguransky, S.; Grego, T.; Kandasamy, S.; Mitchell, A.; Nuka, G.; Paysan-Lafosse, T.; Qureshi, M.; Raj, S.; et al. The InterPro protein families and domains database: 20 years on. *Nucleic Acids Res.* **2021**, *49*, D344–D354. [CrossRef] [PubMed]
104. Zhou, Z.; Liu, Y.; Xu, W.; Pan, J.; Luo, Z.-H.; Li, M. Genome- and Community-Level Interaction Insights into Carbon Utilization and Element Cycling Functions of Hydrothermarchaeota in Hydrothermal Sediment. *mSystems* **2020**, *5*. [CrossRef] [PubMed]
105. Nakahara, N.; Nobu, M.K.; Takaki, Y.; Miyazaki, M.; Tasumi, E.; Sakai, S.; Ogawara, M.; Yoshida, N.; Tamaki, H.; Yamanaka, Y.; et al. *Aggregatilinea lenta* gen. nov., sp. nov., a slow-growing, facultatively anaerobic bacterium isolated from subseafloor sediment, and proposal of the new order *Aggregatilineales* ord. nov. within the class Anaerolineae of the phylum Chloroflexi. *Int. J. Syst. Evol. Microbiol.* **2019**, *69*, 1185–1194. [CrossRef] [PubMed]
106. Anantharaman, K.; Brown, C.T.; Hug, L.A.; Sharon, I.; Castelle, C.J.; Probst, A.J.; Thomas, B.C.; Singh, A.; Wilkins, M.J.; Karaoz, U.; et al. Thousands of microbial genomes shed light on interconnected biogeochemical processes in an aquifer system. *Nat. Commun.* **2016**, *7*, 13219. [CrossRef]
107. Lawson, C.E.; Wu, S.; Bhattacharjee, A.S.; Hamilton, J.J.; McMahon, K.D.; Goel, R.; Noguera, D.R. Metabolic network analysis reveals microbial community interactions in anammox granules. *Nat. Commun.* **2017**, *8*, 15416. [CrossRef] [PubMed]

108. Zhao, Y.; Liu, S.; Jiang, B.; Feng, Y.; Zhu, T.; Tao, H.-C.; Tang, X.; Liu, S. Genome-Centered Metagenomics Analysis Reveals the Symbiotic Organisms Possessing Ability to Cross-Feed with Anammox Bacteria in Anammox Consortia. *Environ. Sci. Technol.* **2018**, *52*, 11285–11296. [[CrossRef](#)]
109. Kato, S.; Sakai, S.; Hirai, M.; Tasumi, E.; Nishizawa, M.; Suzuki, K.; Takai, K. Long-Term Cultivation and Metagenomics Reveal Ecophysiology of Previously Uncultivated Thermophiles Involved in Biogeochemical Nitrogen Cycle. *Microbes Environ.* **2018**, *33*, 107–110. [[CrossRef](#)]
110. Probst, A.J.; Ladd, B.; Jarett, J.K.; Geller-McGrath, D.E.; Sieber, C.M.K.; Emerson, J.B.; Anantharaman, K.; Thomas, B.C.; Malmstrom, R.R.; Stiegelmeyer, M.; et al. Differential depth distribution of microbial function and putative symbionts through sediment-hosted aquifers in the deep terrestrial subsurface. *Nat. Microbiol.* **2018**, *3*, 328–336. [[CrossRef](#)]
111. Parks, D.H.; Chuvochina, M.; Waite, D.W.; Rinke, C.; Skarszewski, A.; Chaumeil, P.A.; Hugenholtz, P. A standardized bacterial taxonomy based on genome phylogeny substantially revises the tree of life. *Nat. Biotechnol.* **2018**, *36*, 996–1004. [[CrossRef](#)]
112. Ali, M.; Shaw, D.R.; Albertsen, M.; Saikaly, P.E. Comparative Genome-Centric Analysis of Freshwater and Marine ANAMMOX Cultures Suggests Functional Redundancy in Nitrogen Removal Processes. *Front. Microbiol.* **2020**, *11*, 1637. [[CrossRef](#)]
113. Campanaro, S.; Treu, L.; Rodriguez-R, L.M.; Kovalovszki, A.; Ziels, R.M.; Maus, I.; Zhu, X.; Kougias, P.G.; Basile, A.; Luo, G.; et al. New insights from the biogas microbiome by comprehensive genome-resolved metagenomics of nearly 1600 species originating from multiple anaerobic digesters. *Biotechnol. Biofuels* **2020**, *13*, 1–18. [[CrossRef](#)]
114. He, C.; Keren, R.; Whittaker, M.L.; Farag, I.F.; Doudna, J.A.; Cate, J.H.D.; Banfield, J.F. Genome-resolved metagenomics reveals site-specific diversity of episymbiotic CPR bacteria and DPANN archaea in groundwater ecosystems. *Nat. Microbiol.* **2021**, *6*, 354–365. [[CrossRef](#)] [[PubMed](#)]
115. Singleton, C.M.; Petriglieri, F.; Kristensen, J.M.; Kirkegaard, R.H.; Michaelsen, T.Y.; Andersen, M.H.; Kondrotaite, Z.; Karst, S.M.; Dueholm, M.S.; Nielsen, P.H.; et al. Connecting structure to function with the recovery of over 1000 high-quality metagenome-assembled genomes from activated sludge using long-read sequencing. *Nat. Commun.* **2021**, *12*, 1–13. [[CrossRef](#)] [[PubMed](#)]
116. Okubo, T.; Toyoda, A.; Fukuhara, K.; Uchiyama, I.; Harigaya, Y.; Kuroiwa, M.; Suzuki, T.; Murakami, Y.; Suwa, Y.; Takami, H. The physiological potential of anammox bacteria as revealed by their core genome structure. *DNA Res.* **2021**, *28*, 28. [[CrossRef](#)] [[PubMed](#)]
117. Philippot, L. Denitrifying genes in bacterial and Archaeal genomes. *Biochim. Biophys. Acta Gene Struct. Expr.* **2002**, *1577*, 355–376. [[CrossRef](#)]
118. Edgar, R.C. Search and clustering orders of magnitude faster than BLAST. *Bioinformatics* **2010**, *26*, 2460–2461. [[CrossRef](#)]
119. Price, M.N.; Dehal, P.S.; Arkin, A.P. FastTree 2—Approximately Maximum-Likelihood Trees for Large Alignments. *PLoS ONE* **2010**, *5*, e9490. [[CrossRef](#)]
120. Rambaut, A. *FigTree v1.4.4*; The Institute of Evolutionary Biology: Edinburgh, UK, 2018.
121. Fu, L.; Niu, B.; Zhu, Z.; Wu, S.; Li, W. CD-HIT: Accelerated for clustering the next-generation sequencing data. *Bioinformatics* **2012**, *28*, 3150–3152. [[CrossRef](#)]
122. Merrick, M.J.; Edwards, R.A. Nitrogen Control in Bacteria. *Microbiol. Mol. Biol. Rev.* **1995**, *59*, 604–622. [[CrossRef](#)]
123. Ninfa, A.J.; Jiang, P.; Atkinson, M.R.; Peliska, J.A. Integration of antagonistic signals in the regulation of nitrogen assimilation in *Escherichia coli*. In *Current Topics in Cellular Regulation*; Stadtman, E.R., Chock, P.B., Eds.; Academic Press: Cambridge, MA, USA, 2001; p. 31-I. Volume 36.
124. Palmer, T.; Santini, C.-L.; Iobbi-Nivol, C.; Eaves, D.J.; Boxer, D.H.; Giordano, G. Involvement of the narJ and mob gene products in distinct steps in the biosynthesis of the molybdoenzyme nitrate reductase in *Escherichia coli*. *Mol. Microbiol.* **1996**, *20*, 875–884. [[CrossRef](#)] [[PubMed](#)]
125. Lake, M.W.; Temple, C.A.; Rajagopalan, K.V.; Schindelin, H. The Crystal Structure of the *Escherichia coli* MobA Protein Provides Insight into Molybdopterin Guanine Dinucleotide Biosynthesis. *J. Biol. Chem.* **2000**, *275*, 40211–40217. [[CrossRef](#)]
126. Guse, A.; Stevenson, C.E.M.; Kuper, J.; Buchanan, G.; Schwarz, G.; Giordano, G.; Magalon, A.; Mendel, R.R.; Lawson, D.M.; Palmer, T. Biochemical and Structural Analysis of the Molybdenum Cofactor Biosynthesis Protein MobA. *J. Biol. Chem.* **2003**, *278*, 25302–25307. [[CrossRef](#)]
127. Hover, B.M.; Tonthat, N.K.; Schumacher, M.A.; Yokoyama, K. Mechanism of pyranopterin ring formation in molybdenum cofactor biosynthesis. *Proc. Natl. Acad. Sci. USA* **2015**, *112*, 6347–6352. [[CrossRef](#)]
128. Richardson, D.J.; Berks, B.; Russell, D.A.; Spiro, S.; Taylor, C.J. Functional, biochemical and genetic diversity of prokaryotic nitrate reductases. *Cell. Mol. Life Sci.* **2001**, *58*, 165–178. [[CrossRef](#)] [[PubMed](#)]
129. Bertero, M.G.; Rothery, R.A.; Palak, M.; Hou, C.; Lim, D.; Blasco, F.; Weiner, J.H.; Strynadka, N.C.J. Insights into the respiratory electron transfer pathway from the structure of nitrate reductase A. *Nat. Struct. Mol. Biol.* **2003**, *10*, 681–687. [[CrossRef](#)]
130. Källberg, M.; Wang, H.; Wang, S.; Peng, J.; Wang, Z.; Lu, H.; Xu, J. Template-based protein structure modeling using the RaptorX web server. *Nat. Protoc.* **2012**, *7*, 1511–1522. [[CrossRef](#)] [[PubMed](#)]
131. Waterhouse, A.; Bertoni, M.; Bienert, S.; Studer, G.; Tauriello, G.; Gumieny, R.; Heer, F.T.; de Beer, T.A.P.; Remppfer, C.; Bordoli, L.; et al. SWISS-MODEL: Homology modelling of protein structures and complexes. *Nucleic Acids Res.* **2018**, *46*, W296–W303. [[CrossRef](#)]
132. Rivera-Cancel, G.; Ko, W.-H.; Tomchick, D.R.; Correa, F.; Gardner, K.H. Full-length structure of a monomeric histidine kinase reveals basis for sensory regulation. *Proc. Natl. Acad. Sci. USA* **2014**, *111*, 17839–17844. [[CrossRef](#)]

133. Diensthuber, R.P.; Bommer, M.; Gleichmann, T.; Möglich, A. Full-Length Structure of a Sensor Histidine Kinase Pinpoints Coaxial Coiled Coils as Signal Transducers and Modulators. *Structure* **2013**, *21*, 1127–1136. [[CrossRef](#)]
134. Orekhov, P.; Bothé, A.; Steinhoff, H.; Shaitan, K.V.; Raunser, S.; Fotiadis, D.; Schlesinger, R.; Klare, J.P.; Engelhard, M. Sensory Rhodopsin I and Sensory Rhodopsin II Form Trimers of Dimers in Complex with their Cognate Transducers. *Photochem. Photobiol.* **2017**, *93*, 796–804. [[CrossRef](#)]
135. Yang, W.; Cassidy, K.; Ames, P.; Diebold, C.A.; Schulten, K.; Luthey-Schulten, Z.; Parkinson, J.S.; Briegel, A. In Situ Conformational Changes of the *Escherichia coli* Serine Chemoreceptor in Different Signaling States. *mBio* **2019**, *10*, e00973-19. [[CrossRef](#)]
136. Cassidy, C.K.; Himes, B.A.; Sun, D.; Ma, J.; Zhao, G.; Parkinson, J.S.; Stansfeld, P.J.; Luthey-Schulten, Z.; Zhang, P. Structure and dynamics of the *E. coli* chemotaxis core signaling complex by cryo-electron tomography and molecular simulations. *Commun. Biol.* **2020**, *3*, 1–10. [[CrossRef](#)]
137. Burt, A.; Cassidy, C.K.; Ames, P.; Bacia-Verloop, M.; Baulard, M.; Huard, K.; Luthey-Schulten, Z.; Desfosses, A.; Stansfeld, P.J.; Margolin, W.; et al. Complete structure of the chemosensory array core signalling unit in an *E. coli* minicell strain. *Nat. Commun.* **2020**, *11*, 1–9. [[CrossRef](#)]
138. Martín-Mora, D.; Fernández, M.; Velando, F.; Ortega, Á.; Gavira, J.A.; Matilla, M.A.; Krell, T. Functional Annotation of Bacterial Signal Transduction Systems: Progress and Challenges. *Int. J. Mol. Sci.* **2018**, *19*, 3755. [[CrossRef](#)]
139. Cheung, J.; Hendrickson, W.A. Structural Analysis of Ligand Stimulation of the Histidine Kinase NarX. *Structure* **2009**, *17*, 190–201. [[CrossRef](#)]
140. Gushchin, I.; Melnikov, I.; Polovinkin, V.; Ishchenko, A.; Yuzhakova, A.; Buslaev, P.; Bourenkov, G.; Grudinin, S.; Round, E.; Balandin, T.; et al. Mechanism of transmembrane signaling by sensor histidine kinases. *Science* **2017**, *356*, eaah6345. [[CrossRef](#)] [[PubMed](#)]
141. Gushchin, I.; Orekhov, P.; Melnikov, I.; Polovinkin, V.; Yuzhakova, A.; Gordeliy, V. Sensor Histidine Kinase NarQ Activates via Helical Rotation, Diagonal Scissoring, and Eventually Piston-Like Shifts. *Int. J. Mol. Sci.* **2020**, *21*, 3110. [[CrossRef](#)] [[PubMed](#)]
142. Cavicchioli, R.; Chiang, R.C.; Kalman, L.V.; Gunsalus, R.P. Role of the periplasmic domain of the *Escherichia coli* NarX sensor-transmitter protein in nitrate-dependent signal transduction and gene regulation. *Mol. Microbiol.* **1996**, *21*, 901–911. [[CrossRef](#)]
143. Chiang, R.C.; Cavicchioli, R.; Gunsalus, R.P. “Locked-on” and “Locked-off” Signal Transduction Mutations in the Periplasmic Domain of the *Escherichia Coli* NarQ and NarX Sensors Affect Nitrate- and Nitrite-Dependent Regulation by NarL and NarP. *Mol. Microbiol.* **1997**, *24*, 1049–1060. [[CrossRef](#)]
144. Williams, S.B.; Stewart, V. Discrimination between structurally related ligands nitrate and nitrite controls autokinase activity of the NarX transmembrane signal transducer of *Escherichia coli* K-12. *Mol. Microbiol.* **1997**, *26*, 911–925. [[CrossRef](#)] [[PubMed](#)]
145. Carpenter, E.P.; Beis, K.; Cameron, A.D.; Iwata, S. Overcoming the challenges of membrane protein crystallography. *Curr. Opin. Struct. Biol.* **2008**, *18*, 581–586. [[CrossRef](#)] [[PubMed](#)]
146. Vinothkumar, K.R.; Henderson, R. Structures of membrane proteins. *Q. Rev. Biophys.* **2010**, *43*, 65–158. [[CrossRef](#)]
147. Bill, R.M.; Henderson, P.J.F.; Iwata, S.; Kunji, E.R.S.; Michel, H.; Neutze, R.; Newstead, S.; Poolman, B.; Tate, C.; Vogel, H. Overcoming barriers to membrane protein structure determination. *Nat. Biotechnol.* **2011**, *29*, 335–340. [[CrossRef](#)] [[PubMed](#)]
148. Li, F.; Egea, P.F.; Vecchio, A.J.; Asial, I.; Gupta, M.; Paulino, J.; Bajaj, R.; Dickinson, M.S.; Ferguson-Miller, S.; Monk, B.C.; et al. Highlighting membrane protein structure and function: A celebration of the Protein Data Bank. *J. Biol. Chem.* **2021**, *296*, 100557. [[CrossRef](#)]
149. Gordeliy, V.I.; Labahn, J.; Moukhametzianov, R.; Efremov, R.; Granzin, J.; Schlesinger, R.; Büldt, G.; Savopol, T.; Scheidig, A.J.; Klare, J.P.; et al. Molecular basis of transmembrane signalling by sensory rhodopsin II–transducer complex. *Nat. Cell Biol.* **2002**, *419*, 484–487. [[CrossRef](#)] [[PubMed](#)]
150. Moukhametzianov, R.; Klare, J.P.; Efremov, R.; Baeken, C.; Göppner, A.; Labahn, J.; Engelhard, M.; Büldt, G.; Gordeliy, V.I. Development of the signal in sensory rhodopsin and its transfer to the cognate transducer. *Nat. Cell Biol.* **2006**, *440*, 115–119. [[CrossRef](#)] [[PubMed](#)]
151. Ishchenko, A.; Round, E.; Borshchevskiy, V.; Grudinin, S.; Gushchin, I.; Klare, J.P.; Remeeva, A.; Polovinkin, V.; Utrobin, P.; Balandin, T.; et al. New Insights on Signal Propagation by Sensory Rhodopsin II/Transducer Complex. *Sci. Rep.* **2017**, *7*, srep41811. [[CrossRef](#)] [[PubMed](#)]
152. Maslenikov, I.; Klammt, C.; Hwang, E.; Kefala, G.; Okamura, M.; Esquivies, L.; Mörs, K.; Glaubitz, C.; Kwiatkowski, W.; Jeon, Y.H.; et al. Membrane domain structures of three classes of histidine kinase receptors by cell-free expression and rapid NMR analysis. *Proc. Natl. Acad. Sci. USA* **2010**, *107*, 10902–10907. [[CrossRef](#)]
153. Molnar, K.S.; Bonomi, M.; Pellarin, R.; Clinthorne, G.D.; Gonzalez, G.; Goldberg, S.D.; Goulian, M.; Sali, A.; DeGrado, W.F. Cys-Scanning Disulfide Crosslinking and Bayesian Modeling Probe the Transmembrane Signaling Mechanism of the Histidine Kinase, PhoQ. *Structure* **2014**, *22*, 1239–1251. [[CrossRef](#)] [[PubMed](#)]
154. Orekhov, P.S.; Klose, D.; Mulkidjanian, A.; Shaitan, K.V.; Engelhard, M.; Klare, J.P.; Steinhoff, H.-J. Signaling and Adaptation Modulate the Dynamics of the Photosensoric Complex of *Natronomonas pharaonis*. *PLoS Comput. Biol.* **2015**, *11*, e1004561. [[CrossRef](#)]
155. Bhate, M.P.; Lemmin, T.; Kuenze, G.; Mensa, B.; Ganguly, S.; Peters, J.M.; Schmidt, N.; Pelton, J.G.; Gross, C.A.; Meiler, J.; et al. Structure and Function of the Transmembrane Domain of NsaS, an Antibiotic Sensing Histidine Kinase in *Staphylococcus aureus*. *J. Am. Chem. Soc.* **2018**, *140*, 7471–7485. [[CrossRef](#)]

156. Szurmant, H.; Bu, L.; Brooks, C.L.; Hoch, J.A. An essential sensor histidine kinase controlled by transmembrane helix interactions with its auxiliary proteins. *Proc. Natl. Acad. Sci. USA* **2008**, *105*, 5891–5896. [[CrossRef](#)] [[PubMed](#)]
157. Russ, W.P.; Engelman, D.M. The GxxxG motif: A framework for transmembrane helix-helix association. *J. Mol. Biol.* **2000**, *296*, 911–919. [[CrossRef](#)]
158. Teese, M.G.; Langosch, D. Role of GxxxG Motifs in Transmembrane Domain Interactions. *Biochemistry* **2015**, *54*, 5125–5135. [[CrossRef](#)]
159. Dawson, J.P.; Weinger, J.S.; Engelman, D.M. Motifs of serine and threonine can drive association of transmembrane helices. *J. Mol. Biol.* **2002**, *316*, 799–805. [[CrossRef](#)]
160. Senes, A.; Engel, D.E.; DeGrado, W.F. Folding of helical membrane proteins: The role of polar, GxxxG-like and proline motifs. *Curr. Opin. Struct. Biol.* **2004**, *14*, 465–479. [[CrossRef](#)]
161. Stopp, M.; Steinmetz, P.A.; Schubert, C.; Griesinger, C.; Schneider, D.; Unden, G. Transmembrane signaling and cytoplasmic signal conversion by dimeric transmembrane helix 2 and a linker domain of the DcuS sensor kinase. *J. Biol. Chem.* **2021**, *296*, 100148. [[CrossRef](#)]
162. Goldberg, S.D.; Clinthorne, G.D.; Goulian, M.; DeGrado, W.F. Transmembrane polar interactions are required for signaling in the *Escherichia coli* sensor kinase PhoQ. *Proc. Natl. Acad. Sci. USA* **2010**, *107*, 8141–8146. [[CrossRef](#)]
163. Lemmin, T.; Soto, C.S.; Clinthorne, G.; DeGrado, W.F.; Peraro, M.D. Assembly of the Transmembrane Domain of *E. coli* PhoQ Histidine Kinase: Implications for Signal Transduction from Molecular Simulations. *PLoS Comput. Biol.* **2013**, *9*, e1002878. [[CrossRef](#)]
164. Aravind, L.; Ponting, C.P. The cytoplasmic helical linker domain of receptor histidine kinase and methyl-accepting proteins is common to many prokaryotic signalling proteins. *FEMS Microbiol. Lett.* **1999**, *176*, 111–116. [[CrossRef](#)]
165. Hulkó, M.; Berndt, F.; Gruber, M.; Linder, J.U.; Truffault, V.; Schultz, A.; Martin, J.; Schultz, J.E.; Lupas, A.N.; Coles, M. The HAMP Domain Structure Implies Helix Rotation in Transmembrane Signaling. *Cell* **2006**, *126*, 929–940. [[CrossRef](#)]
166. Airola, M.V.; Watts, K.J.; Bilwes, A.M.; Crane, B.R. Structure of Concatenated HAMP Domains Provides a Mechanism for Signal Transduction. *Structure* **2010**, *18*, 436–448. [[CrossRef](#)]
167. Wang, C.; Sang, J.; Wang, J.; Su, M.; Downey, J.S.; Wu, Q.; Wang, S.; Cai, Y.; Xu, X.; Wu, J.; et al. Mechanistic Insights Revealed by the Crystal Structure of a Histidine Kinase with Signal Transducer and Sensor Domains. *PLoS Biol.* **2013**, *11*, e1001493. [[CrossRef](#)]
168. Mechaly, A.E.; Sassoon, N.; Betton, J.-M.; Alzari, P.M. Segmental Helical Motions and Dynamical Asymmetry Modulate Histidine Kinase Autophosphorylation. *PLoS Biol.* **2014**, *12*, e1001776. [[CrossRef](#)] [[PubMed](#)]
169. Gushchin, I.Y.; Gordeliy, V.I.; Grudinin, S. Role of the HAMP Domain Region of Sensory Rhodopsin Transducers in Signal Transduction. *Biochemistry* **2011**, *50*, 574–580. [[CrossRef](#)] [[PubMed](#)]
170. Park, H.; Im, W.; Seok, C. Transmembrane Signaling of Chemotaxis Receptor Tar: Insights from Molecular Dynamics Simulation Studies. *Biophys. J.* **2011**, *100*, 2955–2963. [[CrossRef](#)]
171. Gushchin, I.; Gordeliy, V.; Grudinin, S. Two Distinct States of the HAMP Domain from Sensory Rhodopsin Transducer Observed in Unbiased Molecular Dynamics Simulations. *PLoS ONE* **2013**, *8*, e66917. [[CrossRef](#)] [[PubMed](#)]
172. Matamouros, S.; Hager, K.R.; Miller, S.I. HAMP Domain Rotation and Tilting Movements Associated with Signal Transduction in the PhoQ Sensor Kinase. *mBio* **2015**, *6*, e00616-15. [[CrossRef](#)] [[PubMed](#)]
173. Appleman, J.A.; Stewart, V. Mutational Analysis of a Conserved Signal-Transducing Element: The HAMP Linker of the *Escherichia coli* Nitrate Sensor NarX. *J. Bacteriol.* **2003**, *185*, 89–97. [[CrossRef](#)] [[PubMed](#)]
174. Ames, P.; Zhou, Q.; Parkinson, J.S. Mutational Analysis of the Connector Segment in the HAMP Domain of Tsr, the *Escherichia coli* Serine Chemoreceptor. *J. Bacteriol.* **2008**, *190*, 6676–6685. [[CrossRef](#)]
175. Zhou, Q.; Ames, P.; Parkinson, J.S. Mutational analyses of HAMP helices suggest a dynamic bundle model of input-output signalling in chemoreceptors. *Mol. Microbiol.* **2009**, *73*, 801–814. [[CrossRef](#)]
176. Doepper, M.; Bordignon, E.; Klare, J.P.; Holterhues, J.; Martell, S.; Mennes, N.; Li, L.; Engelhard, M.; Steinhoff, H.-J. Salt-driven Equilibrium between Two Conformations in the HAMP Domain from *Natronomonas pharaonis*: The language of signal transfer? *J. Biol. Chem.* **2008**, *283*, 28691–28701. [[CrossRef](#)]
177. Stewart, V. The HAMP signal-conversion domain: Static two-state or dynamic three-state? *Mol. Microbiol.* **2014**, *91*, 853–857. [[CrossRef](#)] [[PubMed](#)]
178. Ames, P.; Zhou, Q.; Parkinson, J.S. HAMP domain structural determinants for signalling and sensory adaptation in Tsr, the *Escherichia coli* serine chemoreceptor. *Mol. Microbiol.* **2013**, *91*, 875–886. [[CrossRef](#)]
179. Wang, B.; Zhao, A.; Novick, R.P.; Muir, T.W. Activation and Inhibition of the Receptor Histidine Kinase AgrC Occurs through Opposite Helical Transduction Motions. *Mol. Cell* **2014**, *53*, 929–940. [[CrossRef](#)] [[PubMed](#)]
180. Lesne, E.; Dupré, E.; Lensink, M.F.; Locht, C.; Antoine, R.; Jacob-Dubuisson, F. Coiled-Coil Antagonism Regulates Activity of Venus Flytrap-Domain-Containing Sensor Kinases of the BvgS Family. *mBio* **2018**, *9*. [[CrossRef](#)]
181. Dupré, E.; Clantin, B.; Yuan, Y.; Lecher, S.; Lesne, E.; Antoine, R.; Villeret, V.; Jacob-Dubuisson, F. Structural insight into the role of the PAS domain for signal transduction in sensor-kinase BvgS. *J. Bacteriol.* **2021**. [[CrossRef](#)]
182. Saita, E.; Abriata, L.A.; Tsai, Y.T.; Trajtenberg, F.; Lemmin, T.; Buschiazzo, A.; Peraro, M.D.; De Mendoza, D.; Albanesi, D. A coiled coil switch mediates cold sensing by the thermosensory protein DesK. *Mol. Microbiol.* **2015**, *98*, 258–271. [[CrossRef](#)]
183. Liu, J.; Yang, J.; Wen, J.; Yang, Y.; Wei, X.; Zhang, X.; Wang, Y.-P. Mutational analysis of dimeric linkers in peri- and cytoplasmic domains of histidine kinase DctB reveals their functional roles in signal transduction. *Open Biol.* **2014**, *4*, 140023. [[CrossRef](#)]

184. Anantharaman, V.; Balaji, S.; Aravind, L. The signaling helix: A common functional theme in diverse signaling proteins. *Biol. Direct* **2006**, *1*, 25. [CrossRef] [PubMed]
185. Bassler, J.; Schultz, J.E.; Lupas, A.N. Adenylate cyclases: Receivers, transducers, and generators of signals. *Cell. Signal.* **2018**, *46*, 135–144. [CrossRef]
186. Shi, R.; McDonald, L.; Cygler, M.; Ekiel, I. Coiled-Coil Helix Rotation Selects Repressing or Activating State of Transcriptional Regulator DhaR. *Structure* **2014**, *22*, 478–487. [CrossRef]
187. Otero, L.H.; Klinke, S.; Rinaldi, J.; Escobar, F.V.; Mroginski, M.A.; López, M.F.; Malamud, F.; Vojnov, A.A.; Hildebrandt, P.; Goldbaum, F.A.; et al. Structure of the Full-Length Bacteriophytochrome from the Plant Pathogen *Xanthomonas campestris* Provides Clues to its Long-Range Signaling Mechanism. *J. Mol. Biol.* **2016**, *428*, 3702–3720. [CrossRef]
188. Gourinchas, G.; Etzl, S.; Göbel, C.; Vide, U.; Madl, T.; Winkler, A. Long-range allosteric signaling in red light-regulated diguanylyl cyclases. *Sci. Adv.* **2017**, *3*, e1602498. [CrossRef] [PubMed]
189. Ferris, H.U.; Dunin-Horkawicz, S.; Hornig, N.; Hulkó, M.; Martin, J.; Schultz, J.E.; Zeth, K.; Lupas, A.N.; Coles, M. Mechanism of Regulation of Receptor Histidine Kinases. *Structure* **2012**, *20*, 56–66. [CrossRef]
190. Ferris, H.U.; Coles, M.; Lupas, A.N.; Hartmann, M.D. Crystallographic snapshot of the *Escherichia coli* EnvZ histidine kinase in an active conformation. *J. Struct. Biol.* **2014**, *186*, 376–379. [CrossRef]
191. Brown, J.H.; Cohen, C.; Parry, D.A. Heptad Breaks in Alpha-Helical Coiled Coils: Stutters and Stammers. *Proteins* **1996**, *26*, 134–145. [CrossRef]
192. Schmidt, N.W.; Grigoryan, G.; DeGrado, W.F. The accommodation index measures the perturbation associated with insertions and deletions in coiled-coils: Application to understand signaling in histidine kinases. *Protein Sci.* **2017**, *26*, 414–435. [CrossRef] [PubMed]
193. Stewart, V.; Chen, L.-L. The S Helix Mediates Signal Transmission as a HAMP Domain Coiled-Coil Extension in the NarX Nitrate Sensor from *Escherichia coli* K-12. *J. Bacteriol.* **2010**, *192*, 734–745. [CrossRef] [PubMed]
194. Weichsel, A.; Kievenaar, J.A.; Curry, R.; Croft, J.T.; Montfort, W.R. Instability in a coiled-coil signaling helix is conserved for signal transduction in soluble guanylyl cyclase. *Protein Sci.* **2019**, *28*, 1830–1839. [CrossRef]
195. Heikaus, C.C.; Pandit, J.; Klevit, R.E. Cyclic Nucleotide Binding GAF Domains from Phosphodiesterases: Structural and Mechanistic Insights. *Structure* **2009**, *17*, 1551–1557. [CrossRef]
196. Anders, K.; Essen, L.-O. The family of phytochrome-like photoreceptors: Diverse, complex and multi-colored, but very useful. *Curr. Opin. Struct. Biol.* **2015**, *35*, 7–16. [CrossRef]
197. Sardiwal, S.; Kendall, S.; Movahedzadeh, F.; Rison, S.C.; Stoker, N.; Djordjevic, S. A GAF Domain in the Hypoxia/NO-inducible *Mycobacterium tuberculosis* DosS Protein Binds Haem. *J. Mol. Biol.* **2005**, *353*, 929–936. [CrossRef]
198. Kumar, A.; Toledo, J.C.; Patel, R.; Lancaster, J.R.; Steyn, A.J.C. *Mycobacterium tuberculosis* DosS is a redox sensor and DosT is a hypoxia sensor. *Proc. Natl. Acad. Sci. USA* **2007**, *104*, 11568–11573. [CrossRef] [PubMed]
199. Unden, G.; Nilkens, S.; Singenstreu, M. Bacterial sensor kinases using Fe–S cluster binding PAS or GAF domains for O<sub>2</sub>sensing. *Dalton Trans.* **2013**, *42*, 3082–3087. [CrossRef] [PubMed]
200. Lin, Z.; Johnson, L.C.; Weissbach, H.; Brot, N.; Lively, M.O.; Lowther, W.T. Free methionine-(R)-sulfoxide reductase from *Escherichia coli* reveals a new GAF domain function. *Proc. Natl. Acad. Sci. USA* **2007**, *104*, 9597–9602. [CrossRef] [PubMed]
201. El-Gebali, S.; Mistry, J.; Bateman, A.; Eddy, S.R.; Luciani, A.; Potter, S.C.; Qureshi, M.; Richardson, L.J.; Salazar, G.A.; Smart, A.; et al. The Pfam protein families database in 2019. *Nucleic Acids Res.* **2018**, *47*, D427–D432. [CrossRef] [PubMed]
202. Kumar, S.; Gillilan, R.E.; Yernool, D.A. Structure and function of the juxtamembrane GAF domain of potassium biosensor KdpD. *Protein Sci.* **2020**, *29*, 2009–2021. [CrossRef]
203. Shin, H.; Ren, Z.; Zeng, X.; Bandara, S.; Yang, X. Structural basis of molecular logic OR in a dual-sensor histidine kinase. *Proc. Natl. Acad. Sci. USA* **2019**, *116*, 19973–19982. [CrossRef]
204. Martinez, S.E.; Bruder, S.; Schultz, A.; Zheng, N.; Schultz, J.E.; Beavo, J.A.; Linder, J.U. Crystal structure of the tandem GAF domains from a cyanobacterial adenylyl cyclase: Modes of ligand binding and dimerization. *Proc. Natl. Acad. Sci. USA* **2005**, *102*, 3082–3087. [CrossRef]
205. Laub, M.T.; Goulian, M. Specificity in Two-Component Signal Transduction Pathways. *Annu. Rev. Genet.* **2007**, *41*, 121–145. [CrossRef]
206. Casino, P.; Rubio, V.; Marina, A. Structural Insight into Partner Specificity and Phosphoryl Transfer in Two-Component Signal Transduction. *Cell* **2009**, *139*, 325–336. [CrossRef] [PubMed]
207. Podgornaia, A.I.; Casino, P.; Marina, A.; Laub, M.T. Structural basis of a rationally rewired protein-protein interface critical to bacterial signaling. *Structure* **2013**, *21*, 1636–1647. [CrossRef]
208. Trajtenberg, F.; Imelio, J.A.; Machado, M.R.; Larrieux, N.; Martí, M.A.; Obal, G.; Mechaly, A.E.; Buschiazzo, A. Regulation of signaling directionality revealed by 3D snapshots of a kinase: Regulator complex in action. *eLife* **2016**, *5*, e21422. [CrossRef] [PubMed]
209. Grebe, T.W.; Stock, J.B. The Histidine protein kinase superfamily. In *Advances in Microbial Physiology*; Poole, R.K., Ed.; Academic Press: San Diego, CA, USA, 1999; Volume 41, pp. 139–227.
210. Huynh, T.A.; Noriega, C.E.; Stewart, V. Conserved mechanism for sensor phosphatase control of two-component signaling revealed in the nitrate sensor NarX. *Proc. Natl. Acad. Sci. USA* **2010**, *107*, 21140–21145. [CrossRef] [PubMed]

211. Huynh, T.N.; Noriega, C.E.; Stewart, V. Missense substitutions reflecting regulatory control of transmitter phosphatase activity in two-component signalling. *Mol. Microbiol.* **2013**, *88*, 459–472. [[CrossRef](#)]
212. Willett, J.; Kirby, J.R. Genetic and Biochemical Dissection of a HisKA Domain Identifies Residues Required Exclusively for Kinase and Phosphatase Activities. *PLoS Genet.* **2012**, *8*, e1003084. [[CrossRef](#)]
213. Ashenberg, O.; Keating, A.E.; Laub, M.T. Helix Bundle Loops Determine Whether Histidine Kinases Autophosphorylate in cis or in trans. *J. Mol. Biol.* **2013**, *425*, 1198–1209. [[CrossRef](#)]
214. Huynh, T.A.; Chen, L.-L.; Stewart, V. Sensor-response regulator interactions in a cross-regulated signal transduction network. *Microbiology* **2015**, *161*, 1504–1515. [[CrossRef](#)]
215. Albanesi, D.; Martín, M.; Trajtenberg, F.; Mansilla, M.C.; Haouz, A.; Alzari, P.M.; de Mendoza, D.; Buschiazzo, A. Structural plasticity and catalysis regulation of a thermosensor histidine kinase. *Proc. Natl. Acad. Sci. USA* **2009**, *106*, 16185–16190. [[CrossRef](#)]
216. Abriata, L.A.; Albanesi, D.; Peraro, M.D.; De Mendoza, D. Signal Sensing and Transduction by Histidine Kinases as Unveiled through Studies on a Temperature Sensor. *Acc. Chem. Res.* **2017**, *50*, 1359–1366. [[CrossRef](#)]
217. Dutta, R.; Inouye, M. GHKL, an emergent ATPase/kinase superfamily. *Trends Biochem. Sci.* **2000**, *25*, 24–28. [[CrossRef](#)]
218. Tiwari, N.; López-Redondo, M.; Miguel-Romero, L.; Kulhankova, K.; Cahill, M.P.; Tran, P.M.; Kinney, K.J.; Kilgore, S.H.; Al-Tameemi, H.; Herfst, C.A.; et al. The SrrAB two-component system regulates *Staphylococcus aureus* pathogenicity through redox sensitive cysteines. *Proc. Natl. Acad. Sci. USA* **2020**, *117*, 10989–10999. [[CrossRef](#)]
219. Stewart, V.; Chen, L.-L.; Wu, H.-C. Response to culture aeration mediated by the nitrate and nitrite sensor NarQ of *Escherichia coli* K-12. *Mol. Microbiol.* **2003**, *50*, 1391–1399. [[CrossRef](#)] [[PubMed](#)]
220. Paulsen, C.E.; Carroll, K.S. Cysteine-Mediated Redox Signaling: Chemistry, Biology, and Tools for Discovery. *Chem. Rev.* **2013**, *113*, 4633–4679. [[CrossRef](#)] [[PubMed](#)]
221. Sevilla, E.; Bes, M.T.; González, A.; Peleato, M.L.; Fillat, M.F. Redox-Based Transcriptional Regulation in Prokaryotes: Revisiting Model Mechanisms. *Antioxid. Redox Signal.* **2019**, *30*, 1651–1696. [[CrossRef](#)] [[PubMed](#)]
222. Valderrama, J.A.; Gómez-Álvarez, H.; Martín-Moldes, Z.; Berbís, M.Á.; Cañada, F.J.; Durante-Rodríguez, G.; Díaz, E. A Novel Redox-Sensing Histidine Kinase That Controls Carbon Catabolite Repression in *Azoarcus* sp. CIB. *mBio* **2019**, *10*. [[CrossRef](#)]
223. Celikel, R.; Veldore, V.H.; Mathews, I.; Devine, K.M.; Varughese, K.I. ATP forms a stable complex with the essential histidine kinase WalK (YycG) domain. *Acta Crystallogr. Sect. D Biol. Crystallogr.* **2012**, *68*, 839–845. [[CrossRef](#)] [[PubMed](#)]